Dermatopathology

437 miR-205 Is Downregulated in Cutaneous Malignant Melanoma
MS Abi Daoud, J Chen, N Zhang, H Feilotter, V Tron. Queen's University, Kingston, ON, Canada.
Background: The molecular mechanisms regulating melanoma progression are not well understood. Deregulation of microRNA (miRNA) expression has been observed in many diseases, including cancer. We speculated that miRNAs are deregulated in malignant melanoma, and specific miRNAs are involved in melanoma tumorigenesis and progression.
Design: To address this, we began by comparing the miRNA expression profiles of benign and malignant human melanocytic lesions, including nevi (n=8), primary melanoma (n=8), and metastatic melanoma (n=9) using archival formalin fixed, paraffin embedded (FFPE) tissue. We have previously confirmed the validity of using FFPE tissue to profile miRNAs using an array platform. The Agilent miRNA microarray platform was used to generate miRNA expression profiles, and Significance Analysis of Microarray (SAM) was applied to identify differentially expressed miRNA. Unsupervised hierarchical clustering was able to separate nevi and melanoma samples. We found both up-regulated and down-regulated miRNAs in melanoma. One of the most significantly down regulated miRNAs in melanoma was miR-205, showing a 0.06 fold change in metastatic melanoma, and a 0.23 fold change in primary melanoma, when compared to the expression in benign nevi. TaqMan qRT-PCR analysis validated the down regulation of miR-205 in melanoma (delta Ct 10.53 ± 1.68) over benign nevus (delta Ct -3.98 ± 0.23), $p \leq 0.007$. To investigate direct downstream targets of miR-205, we performed an in-silico analysis using TargetScan 4.2 software. Two potentially relevant targets to miR-205 were identified, Bcl-2 and c-Kit. A TMA was constructed using the same tumors in which miRNA expression was performed, and immunohistochemistry staining for Bcl-2 and c-Kit conducted. We then ran a Spearman analysis, attempting to show the expected negative correlation between miR-205 array expression levels and protein expression.
Results: A negative correlation was noted between c-Kit expression and miR-205 levels in metastatic melanoma, and not nevi or primary melanoma, but it did not reach significance (-0.268, NS). However, a significant negative correlation was found between miR-205 and Bcl-2 expression in metastatic melanoma samples (-0.818, p≤0.007), but not in nevi or primary melanoma.
Conclusions: Our studies suggest that miR-205 is deregulated in malignant melanoma in a progression specific manner and that miR-205 loss may be linked to increased Bcl-2 expression.

438 Merkel Cell Carcinoma: Correlation of KIT Expression with Survival and Evaluation of KIT Gene Mutational Status
A Andea, R Patel, M Kraemer, S Ponnazhagan, S Kumar, D Jhala, I Eltoum, G Siegal. UAB, Birmingham, AL.
Background: Merkel cell carcinoma (MCC) is one of the most aggressive primary cutaneous malignancies. Currently there is no effective therapy available for disseminated disease. Most MCCs express KIT by immunohistochemistry (IHC). Since relatively little is known regarding the biological significance of KIT in MCC, we aimed to investigate the effects of KIT expression on tumor progression and to assess the presence of activating mutations in the KIT gene which could provide new therapeutic options for MCC similar to gastrointestinal stromal tumors (GIST) and melanomas.
Design: A total of 40 patients with a diagnosis of MCC were identified with a median follow-up interval of 20 months. KIT expression was assessed by IHC on formalin fixed, paraffin embedded material. Cases were divided into low expressors (0-1+ staining intensity) and high expressors (2-3+ staining intensity). Direct sequencing of exons 9, 11, 13, 17, 18 of the KIT gene spanning the extra-cellular, juxtamembrane and tyrosine kinase domains, previously identified as mutation sites in GIST and melanomas, was performed from cases with high KIT expression.
Results: The overall 5-year survival rate was 37%. A total of 30 tumors from 21 patients were analyzed for KIT expression. High expression was seen in 67% of the patients. Five-year survival rates in tumors expressing high versus low levels of KIT were 0% versus 56.4% respectively however, the difference did not reach statistical significance (p=0.1). A total of 18 tumors from 14 patients with high expression were analyzed for mutational status of the KIT gene. Analysis of 216 electropherograms revealed 4 point mutations. Two of these were silent mutations involving exons 17 (c.2394 C>T -2 cases) and 18 (c.2586 G>C -1 case) and 2 involved the flanking 5' intronic region of exon 17 (-107bp T>A -5 cases and -77bp G>A -7 cases). Two of the identified mutations corresponded to previously reported polymorphisms of the KIT gene.
Conclusions: Expression of KIT protein appears to correlate with a worse prognosis in MCC patients raising the possibility of an active role of this receptor in tumor progression and metastasis. We did not identify KIT activating mutations in the 18 tumors analyzed suggesting that alternative mechanisms, possible involving up- or downstream effectors of KIT pathway are involved in the pathogenesis of MCC. Further studies are warranted to elucidate the biologic significance of KIT protein over-expression in MCC and the potential therapeutic value of KIT inhibitors.

439 Correlation of Axillary Skin and Muscle Biopsy Results in Mitochondrial Cytopathy
CE Baran, RA Prayson. Cleveland Clinic Lerner College of Medicine, Cleveland, OH; Cleveland Clinic Foundation, Cleveland, OH.
Background: There is well established, albeit limited, literature documenting the role of axillary skin biopsies (ASB) and skeletal muscle biopsies in the evaluation of metabolic diseases and mitochondrial cytopathy. To our knowledge, no studies have attempted to correlate the results of ASB performed for metabolic diseases and muscle biopsy results, particularly with respect to mitochondrial disorders.

Design: Electron microscopy (EM) files were searched for ASB performed between 1990-2007 for the evaluation of metabolic disease. 536 ASB were performed and comprise the study group. Skin and muscle biopsy (from the same patients (pts)) results, when available, were reviewed to identify mitochondrial alterations.
Results: Of 536 ASB, 64 (11.9%) demonstrated pathologic findings by EM; 31/64 biopsies (48.4%) had mitochondrial abnormalities including large mitochondria (n= 22), expanded matrix material with reduced cristae (n= 21), increased number (n=10), pleomorphism (n=8), lipid droplets (n=3), and presence of dense matrical granules (n=1). 17/31 pts with abnormal mitochondria also had muscle biopsies performed; 7 (41.2%) muscles demonstrated mitochondrial abnormalities including cytochrome oxidase negative fibers (n=2), increased succinate dehydrogenase (SDH) staining (n=2), increased mitochondrial number on EM (n=6), and enlarged mitochondria with abnormal morphology (n=2) on EM. 131/505 pts with normal mitochondria by ASB also had muscle biopsies performed; 58 (44.3%) of these muscles demonstrated mitochondrial abnormalities including increased mitochondrial number (n=45), cytochrome oxidase negative fibers (n=8), increased SDH staining (n=7), ragged red fibers (n=5), and irregular morphology (n=4). Follow-up was available in 26/31 pts with abnormal mitochondria by ASB. A clinical or biochemical diagnosis was reached in 11 pts: electron transport chain abnormalities (n=6), Lennox-Gastaut syndrome (n=1), pyruvate dehydrogenase deficiency (n=1), *Charcot-Marie-Tooth* disease type 1A (n=1), scleroderma (n=1), and cerebral palsy (n=1).
Conclusions: An ASB is helpful in the evaluation of some mitochondrial disorders, but often the findings are nonspecific. A negative biopsy result does not rule out the possibility of a mitochondrial disorder, but a positive result may provide direction for further evaluation. Muscle biopsies add to the diagnostic yield of the ASB in pts suspected of having mitochondrial cytopathy.

440 Mass Spectrometry Based Proteomic Analysis Identifies Two Distinct Types of Cutaneous Amyloidosis
JC Berg, JA Vrana, JD Theis, JD Gamez, TF Flotte, RH Weenig, AH Dogan. Mayo Clinic, Rochester, MN.
Background: Amyloid present in the skin can represent involvement by either a systemic disease or a primary, localized process. While the nonspecific amorphous deposits appear the same by light microscopy, the underlying etiology varies. As the management of amyloidosis targets underlying pathogenesis and may include high risk strategies, accurate classification is a clinical priority. To understand the pathogenesis of cutaneous amyloidosis we utilized a novel microdissection and mass spectrometry based approach to identify two distinct cutaneous amyloid types with characteristic clinico-pathological features.
Design: 15 cases of cutaneous amyloidosis were identified from Mayo Clinic files with corresponding clinical information. In each case, the diagnosis of amyloidosis was confirmed by Congo red reactivity with appropriate color change under polarized light. Amyloid deposits were microdissected, processed and trypsin digested into peptides. The peptides were analyzed by nano-flow liquid chromatography electrospray tandem mass spectrometry (LC-MS/MS). To identify the protein constituents of amyloid deposits, the resulting LC-MS/MS data were correlated to theoretical fragmentation patterns of tryptic peptide sequences from the Swissprot database using Scaffold program. To validate the findings of LC-MS/MS, immunohistochemistry for CK5, CK14, immunoglobulin kappa (IGK) and lambda light chains (IGL), TTR, SAA was performed.
Results: LC MS/MS identified two distinct protein profiles in cutaneous amyloid deposits. In 10 cases the amyloid deposits were enriched in cytokeratin 5 and 14 and, in the remaining 5 cases, peptides representing IGK (4/5) or IGL (1/5) were dominant. SAP was a constituent of both subsets. Interestingly, the cases associated with CK 5 and CK14 amyloid deposition were characterized by pruritis with focal amyloid deposition at the dermal-epidermal junction. None of the patients had clinical evidence of systemic amyloidosis. In contrast, the cases with IGK or IGL deposition lacked a primary skin pathology, but 3 out of 5 had evidence for an underlying systemic plasma cell proliferative disorder.
Conclusions: LC-MS/MS based proteomic analysis of cutaneous amyloidosis identified two distinct cutaneous amyloid types with characteristic clinico-pathological features. Recognition of these two distinct clinico-pathological types of cutaneous amyloidosis is critical in clinical management of these patients.

441 Primary Cutaneous Large B Cell Lymphoma Shows Activation of Nuclear Factor Kappa B with Low Incidence of Epstein Barr Virus
S Bhagavathi, MC Patel, AM Blenc, S Warren, M Amin, RK Malhotra. Indiana University, Indianapolis, IN; William Beaumont Hospital, Royal Oak, MI.
Background: Nuclear factor-kappa B (NF-kB) is a major transcription factors which has been identified as an important factor in the pathogenesis of lymphoma. Constitutive expression of the NF-kB pathway plays a critical role in the lymphomagenesis. In addition, Epstein Barr Virus (EBV) is also known to play an important role in lymphomagenesis and known to carry NF-kB activating oncoproteins. However, the role of NF-kappa B activation and EBV in primary cutaneous diffuse large B-cell lymphoma (PCDLBL), an extranodal non-hodgkin lymphoma confined to the skin at presentation, is largely unknown. The aim of this study is to determine the incidence of NF-kappa B activation and EBV infection in PCDLBL.
Design: We evaluated ten cases of PCDLBL in immunocompetent patients from our institutions between the years 2000 and 2008. A panel of immuoperoxidase stains; CD3, CD10, CD20, BCL2, BCL6, and MUM1 were performed on all cases. In addition, NF-kappa B pathway activation was evaluated using an immunostain for P65. Nuclear staining for P65 is determined as an indicator of activation of NF-kB, irrespective of cytoplasmic staining. The presence or absence of EBV was assessed using EBER in-situ hybridization (ISH) probe. Known prognostic markers in lymphoma such as P53, P16, and MIB1 by immunohistochemical stains were also performed.

Results: All ten cases were CD20 positive and CD3 negative. CD10, BCL6, BCL2, and MUM1 were positive in 4/10 (40%), 6/10 (60%), 7/10 (70%), and 6/10 (60%) cases respectively. NF-kappa B activation as determined by nuclear staining was detected in 7/10 (70%) cases. The remaining cases showed cytoplasmic staining only and hence were determined not to be NF-kB activated. One (10%) case was positive for EBV by ISH. Interestingly, the EBV positive case was also positive for MUM1 and negative for CD10, indicating an activated immunophenotype.

Conclusions: Our study demonstrated activation of the NF-kappa B pathway in a majority (70%) of PCDLBL. Thus, NF-kappa B may be a potential therapeutic target in patients with PCDLBL. Besides NF-kB pathway, the role of other pathways needs further exploration in cases of PCDLBL. Even though the inidence of EBV is low, the exact role of EBV in the pathogenesis of PCDLBL needs further clarification in a study with large patient samples.

442 Diagnostic Value of Sox10 Immunohistochemical Staining for the Detection of Metastatic Melanoma in Sentinel Lymph Nodes
E Blochin, D Nonaka. New York University School of Medicine, New York, NY.
Background: Sox10 is a pan-Schwannian and melanocytic marker superior to S-100 protein for its sensitivity and specificity (Am J Surg Pathol. 2008; 32(9):1291-8). S-100 protein, Melan A, and HMB-45 are commonly used for the detection of metastatic melanomas in the sentinel lymph nodes, with S-100 protein being the most sensitive. S-100 protein, however, can often be expressed by interdigitating dendritic cells and follicular dendritic cells of the lymph nodes. In a majority of cases, metastatic melanomas can be highlighted by a combination of the above three markers. Diagnostic problems may occur when there is no reaction to melanocyte specific markers, as is often the case with spindle cell and desmoplastic melanoma, or melanoma after multiple recurrences.
Design: 121 lymph nodes were studied from 80 consecutive sentinel lymphadenectomy procedures. Our protocol for melanoma sentinel lymph node work-up is comprised of 17 consecutive sections for each block, with H&E staining on the 1st, 5th, 9th, 13th and 17th sections, and S-100 protein, HMB-45, and Melan A immunostaining on the 2nd, 6th and 10th sections. This procedure yielded 33 lymph nodes positive for metastatic melanoma (PLNs) and 88 melanoma-negative lymph nodes (NLNs). After completion of this diagnostic work-up, Sox10 was stained on the 7th section in all lymph nodes. The extent of staining was graded as follows: 1+, 1-25%; 2+, 25-50%; 3+, 50-75%; 4+, ≥ 75%.
Results: Diffuse (4+) Sox10 nuclear expression was seen in metastatic melanomas of all 33 PLNs (100%) while no melanoma was newly detected by Sox10 staining in any of the 88 NLNs. Melan A and HMB-45 were expressed in 29 (88%) and 27 (82%) of the lymph nodes. S-100 protein expression was detected without difficulty in 29 PLNs with 4+, 3+ and 1+ in 26, 2 and 1 lymph nodes. The remaining four lymph nodes contained a few HMB-45 and Melan A-positive single melanoma cells, which were, on S-100 protein stained slides, completely obscured by extensive S-100 protein-reactive dendritic cell population, but Sox10 highlighted these melanoma cells but not the dendritic cells. Metastatic desmoplastic melanoma in one lymph node was positive for Sox10 and S-100 protein, but negative for Melan A and HMB-45. Capsular nevus in three of the lymph nodes showed positive reaction to Sox10, S-100 protein, and Melan A, but not to HMB-45.
Conclusions: Owing to its excellent specificity and sensitivity Sox10 can replace the conventional panel of immunostains and be solely used for sentinel lymphadenectomy specimens for melanoma.

443 Rb Is Hyperphosphorylated in Most Merkel Cell Carcinomas
EM Cham, TA Victor, R Orr, M Morgan, KW Lannert, SM Share, TC Pereira, WB Laskin, CD Sturgis. North Shore University Health System, Evanston, IL; Allegheny General Hospital, Pittsburgh, PA; Northwestern University Feinberg School of Medicine, Chicago, IL; CellNetix, Seattle, WA.
Background: Merkel cell carcinoma (MCC) is an aggressive skin tumor with epithelial and neuroendocrine differentiation. MCC oncogenesis is not well understood, but may involve polyomavirus (PyV) mediated dysregulation of the retinoblastoma (Rb) pathway. Rb controls cell cycle progression. During cell transition from G1 to S phase, Rb is converted from a hypo- to hyperphosphorylated state. Previously, we showed that p16, an upstream regulator of Rb, is overexpressed in nearly all MCCs. The aim of our study is to characterize the expression pattern of Rb in MCCs.
Design: 45 specimens from 34 patients obtained from 3 institutions' archives (NSUHS 1992-2007, NWMH 2000-2006, AGH 1994-2005), included 28 primary, 11 metastatic, 5 recurrent, and 1 MCC without available info. There were 27 (60%) males, 17 (38%) females, and 1 patient without available info. Mean age was 60 years (44-94 years). A tissue microarray with 3 to 5 cores (0.6 mm) of each MCC was made. Anti-human phospho-Rb (pRb, conc. polyclonal antibody, 1:500, Cell Signaling Technology) IHC was done with antigen retrieval (decloaking chamber, Biocare Medical). Results for pRb staining were interpreted by EMC and scored on a semiquantitative 4-tiered scale.
Results: Nuclear and/or cytoplasmic reactivity for pRb was seen in 83% (37 of 45) of the MCCs. 76% (22 of 29) of primary, 91% (10 of 11) of metastatic, and 80% (4 of 5) of recurrent MCCs showed nuclear and/or cytoplasmic staining in varying intensities. Of the 37 MCCs positive for pRb, 22, 11, and 4 had nuclear only, nuclear + cytoplasmic, and cytoplasmic only staining, respectively. Of the 33 MCCs with nuclear staining, 12 and 21 showed strong and weak intensity, respectively. Of the 15 MCCs with cytoplasmic staining, all showed weak intensity.
Conclusions: Our data show most MCCs express pRb in the nucleus and/or cytoplasm. This Rb hyperphosphorylation explains the high proliferation rate seen in many MCCs and why p16 is overexpressed in most MCCs. The pRb expression patterns varied in cellular location, reactivity, and intensity, suggesting multiple mechanisms may be responsible for the Rb dysregulation. PyV transforms cells through deregulation of tumor suppressors such as Rb. Our results are consistent with studies showing that human PyV may play a role in MCC oncogenesis.

444 Histologic Features of Acute Ixodidae Tick Bites: Clues to Pathogenesis of Disease Transmission
MM Chan, L Zhao, SR Tahan. Beth Israel Deaconess Medical Center, Boston, MA, Venezuela; Harvard Medical School, Boston, MA.
Background: It is well-known that tick bites, as those from the *Iodidae* tick, facilitate the transmission of clinically important diseases including Lyme disease, Rocky Mountain Spotted Fever and Bebesiosis. The ability of the tick to remain attached to the skin for days, however, has yet to be elucidated. By comparing the histologic features of acute and remote tick bites, we propose a mechanism by which the tick seemingly evades the host immune response during its prolonged feed.
Design: Skin specimens from fourteen patients who sustained tick bites were examined. Eight histologic sections showed retained tick mouth parts within the epidermis and were, thus, designated as "acute" tick bites. "Remote" tick bites lacked visible tick parts, however, patients reported a history of a tick bite greater than 2 months prior.
Results: Dramatic histologic differences were observed between skin biopsies from patients with acute *versus* remote tick bites. In all *acute* tick bite cases (n=8/8), a necrobiotic collagen core is observed surrounding the tick mouthpart that extends from the epidermis into the deep reticular dermis. The adjacent epidermis shows only mild reactive spongiotic changes. Interstitial neutrophils are seen scattered throughout the reticular dermis, yet are absent near and within the necrobiotic core. Extensive eosinophilic hyaline thrombi are seen in dermal and subcutaneous arterioles. In contrast, the skin sections of remote tick bites (n=6) show a prominent superficial to deep dermal and subcutaneous lymphocytic infiltrate with abundant admixed eosinophils suggesting a prolonged dermal hypersensitivity reaction. Two of these cases exhibited marked reactive lymphoid hyperplasia with germinal center formation. Necrobiotic collagen and eosinophilic hyaline thrombi were not seen in these remote tick bites.
Conclusions: This data represents findings from one of the largest reported series of acute tick bites to date. The tick appears to induce collagen necrobiosis which surrounds the tick mouth parts and prevents access by inflammatory cells. In addition, through induction of a localized coagulopathy, arteriole thrombi are formed that block leukocyte margination and chemotaxis. The pathologic mechanism of these changes is not understood, however the the tick appears to create an immune-protected environment capable of enhancing disease transmission.

445 Superficial Micronodules of Pregnancy (SMOPs) and MIB-1 (Ki-67) Proliferation Index in Benign Nevi Excised during Pregnancy
MP Chan, MM Chan, SR Tahan. Beth Israel Deaconess Medical Center, Boston, MA.
Background: The clinical appearance of benign nevi can dramatically change during pregnancy, leading to concern for malignant transformation and excisional biopsy. Because the hormonal milieu of pregnancy has not been shown to alter the banal behavior of these nevi, histologic characterization is needed to prevent overdiagnosis and unnecessary treatment. In this study we evaluate the histology of banal nevi removed during pregnancy, assess proliferative activity, and identify distinct histologic features.
Design: Dermal nevi excised from pregnant women during the second and third trimesters (n=10) were compared with location- and aged-matched controls (n=10) in a blinded manner. Immunohistochemical stain for MIB-1 (Ki-67) was performed on paraffin sections. A unique histologic entity is described—*superficial micronodules of pregnancy* (SMOPs)—as cytologically distinctive rounded clusters of plump epithelioid melanocytes with abundant cytoplasm and prominent nucleoli, present in the superficial aspect of the nevus. Other features including mitoses, multinucleated melanocytes, and pigmentation (graded from 0-3) were also examined.
Results: The average age (32.2 ± 2.4 and 29.5 ± 5.6 years, pregnant vs. control, respectively) and nevic location (trunk, head and neck) are similar between groups. Intraepidermal cytologic atypia is minimal. Histologic features are summarized below:

	# Dermal mitoses / 10 hpf	MIB-1 (% positive)	Presence of SMOPs	Multinucleated melanocytes	Amount of pigmentation
Pregnant (n=10)	2.5 (±1.96)	3.5 (±3.66)	8/10	0/10	1.3
Control (n=10)	0.2 (±0.63)	1.0 (±1.8)	3/10	5/10	1.1
P-value	0.002	0.081	0.025	0.010	0.630

Benign dermal nevi excised during pregnancy have increased mitotic figures, are more likely to have SMOPs, and lack multinucleated dermal melanocytes. There is a trend towards higher MIB-1 activity in the nevi of pregnancy, although not statistically significant.
Conclusions: Benign dermal nevi of pregnancy demonstrate characteristic histologic features including *superficial micronodules of pregnancy* (SMOPs), increased dermal mitotic figures, and increased MIB-1 proliferation index. The disproportional increase in observed mitotic figures compared to MIB-1 may suggest a hormonal effect on cell cycle regulation.

446 Clusterin Expression Correlates with Tumor Progression in Mycosis Fungoides
P Chandra, Z Zuo, JA Plaza, H Koeppen, AH Diwan, LJ Medeiros, VG Prieto. University of Texas MD Anderson Cancer Center, Houston, TX; Medical College of Wisconsin, Milwaukee, WI.
Background: Clusterin is a ubiquitously expressed glycoprotein and a diagnostic marker of anaplastic large cell lymphoma (ALCL). Mycosis fungoides (MF) with progression to large cell transformation (LCT) may histologically resemble ALCL. We therefore evaluated clusterin expression in MF and compared the results with clinical stage and number of large cells. We also assessed morphologically similar cutaneous T-cell lymphoproliferative disorders (T-LPD).

Design: Paraffin blocks of 97 cutaneous T-LPD specimens were identified including 70 cases of MF (19 patch, 28 plaque, 21 tumor stage, and 2 with erythroderma), 18 ALCL (16 cutaneous and 2 systemic), 6 peripheral T-cell lymphomas (PTCL), and 3 lymphomatoid papulosis (Lyp). Cases were classified according to World Health Organization criteria. Cases of MF with increased large cells (MF-LC) had greater than 10% but less than 25% large cells. Cases of MF in large cell transformation (MF-LCT) had at least 25% large cells. Clusterin expression was assessed using immunohistochemical methods on prepared unstained tissue sections. A case was scored as positive when at least 5% of the infiltrate expressed clusterin. Statistical differences were calculated using Chi-squared analysis.

Results: Clusterin was positive in 36/70 (51%) of MF specimens. Expression was noted by both small and large lymphocytes and stromal cells. According to clinical stage, 3/19 (16%) patch, 13/28 (46%) plaque, and 20/23 (87%) tumors/erythroderma were clusterin positive. Histologically, 43% of MF cases showed predominantly small cells, 26% were MF-LC, and 31% were MF-LCT. According to cytologic composition, 6/30 (20%) small cell MF were clusterin positive versus 12/18 (67%) MF-LC and 18/22 (82%) MF-LCT. With the exception of MF-LC versus MF-LCT, differences in clusterin expression were statistically significant (p less than 0.0001 to 0.03). Clusterin was also positive in all cases of LyP and systemic ALCL, 7/16 (43%) cases of cutaneous ALCL, and 1/6 cases of PTCL (17%).

Conclusions: Clusterin expression is common in MF, ALCL, and Lyp and uncommon in PTCL. In MF, clusterin expression correlates with clinical stage and increased large cells.

---

447 The $BRAF^{V600E}$ Mutation Induces Blue Nevi, Epithelioid Melanocytoma and Malignant Peripheral Nerve Sheath Tumour-Like Malignant Melanoma in Mice
N Dhomen, FC Geyer, R Hayward, JS Reis-Filho, R Marais. Institute of Cancer Research, London, United Kingdom.

Background: Several genetic alterations have been described in human melanomas, of which *BRAF* activating mutations are seen in 50-70% of the cases. The most prevalent mutation is V600E, which leads to the substitution of a glutamic acid for valine at position 600. $BRAF^{V600E}$ has been shown to drive proliferation *in vitro* and tumour maintenance and progression *in vivo*, suggesting it is a potent oncogene. Our aim was to investigate the role of $BRAF^{V600E}$ in melanomagenesis using an engineered mouse model where this mutation was specifically introduced in melanocytes.

Design: Using a Cre recombinase-based system, we have developed a mouse model of melanoma, driven by oncogenic *Braf*. Topical administration of tamoxifen results in a recombination event causing $Braf^{V600E}$ to be expressed specifically in melanocytes. Selected lesions were subjected to immunohistochemical analysis with antibodies against S100 protein and reverse transcriptase PCR (RT-PCR) for M-Mitf, Sox10, Pax3, c-kit, tyrosinase and Trp2.

Results: $Braf^{V600E}$ induced skin hyper-pigmentation and the progressive development of melanocytic lesions. 100% of the mice had multiple blue naevi throughout the body and 80% further developed large, dark and asymmetrical lesions in the eyelids and/or perianal areas, with morphological features consistent with the diagnosis of pigmented epithelioid melanocytoma. Finally, $Braf^{V600E}$ induced rapidly growing, infiltrating and destructive, oligomelanotic/amelanotic spindle cell tumours in 60-70% of the mice. Results of histopathological, immunohistochemical and RT-PCR analysis provided strong circumstantial evidence to suggest that these locally aggressive oligomelanotic/amelanotic spindle cell tumours were malignant peripheral nerve sheath tumour-like spindle cell malignant melanomas.

Conclusions: Our model demonstrates that activating $Braf^{V600E}$ mutations in melanocytes of mice lead to the development of lesions that recapitulate the histological and molecular features of benign and malignant human melanocytic neoplasms. Furthermore, this model may help understand the spectrum of blue cell lesions.

---

448 Epidermal Hyperplasia: A Role for Growth Factor Ligand and Receptor Mediated Induction?
BC Dickson, KG Danielson, MA Young, JS Brooks. Pennsylvania Hospital, Philadelphia, PA.

Background: Epidermal hyperplasia (EH) is a benign process characterized by increased thickness of squamous epithelium in a number of clinical entities, including dermatofibroma (DF). Our hypothesis was that one or more growth factor ligands and receptors may be expressed in neoplasms with and without EH.

Design: We tested 15 cases of DF, comparing them to 5 cases of dermatofibrosarcoma protuberans (DFSP). Immunohistochemistry (IHC) was performed on FFPE sections using a panel of antibodies for various markers, including: FGF-2 (1:400; sc-79; Santa Cruz, CA), FGF-3 (1:10; sc80034; Santa Cruz) and IGF-1 (1:10; sc-9013; Santa Cruz); Bek (1:100; sc-122; Santa Cruz), FGFR-3 (1:100; sc-123; Santa Cruz) and IGFR-1 (1:100; sc-81167; Santa Cruz). Cytoplasmic staining was quantified based on the percentage of cells showing immunoreactivity (0-5) for the epidermis (E), neoplasm (N) and dermal fibroblasts (F).

Results: IHC for each of the markers revealed appreciable intra- and inter- group differences in staining. From the summarized scores no consistent relationship with overexpression emerged (Table). Analysis of variance (ANOVA) comparing DF with DFSP demonstrated significantly greater IGFR-1 expression within the epidermis (P<0.005), neoplasm (P<0.005) and dermal fibroblasts (P<0.05) of DF compared to DFSP. There was significantly greater IGF-1 expression within the epidermis of DF compared to DFSP (P<0.05). Finally, there was significantly more FGF-3 produced within the neoplastic cells of DF compared to DFSP (P<0.05).

Lesion	Location	FGF-2	FGF-3	IGF-1	BEK	FGFR-3	IGFR-1
DF	E	2.2	3.4	4.4	1.2	1.8	2.0
	N	3.4	4.0	3.9	2.1	1.4	1.8
	F	3.8	3.2	3.8	2.1	2.0	2.0
DFSP	E	2.3	3.3	3.3	1.3	2.0	1.3
	N	3.8	3.0	3.8	1.8	1.2	1.2
	F	3.8	2.3	3.3	1.8	2.0	1.5

Table: Average score for expression of various growth factors ligands and receptors.

Conclusions: Our analysis of several common growth factors and receptors failed to identify a definitive mechanism responsible for EH in DF. Nevertheless, there is greater IGFR-1 expression in the epidermis, neoplastic cells and fibroblasts of DF compared to DFSP. Why IGF-1 expression is greater in the epidermis is somewhat counterintuitive, but may suggest a possible contribution to EH. It is interesting that statistical significance was also achieved with FGF-3 expression in the neoplastic cells of DF; however, its receptor is not increased in the epidermis, making the relevance of this observation unclear. Thus, EH is likely the result of a complex and interdependant epidermis–neoplasm relationship.

---

449 Detection of 'Merkel Cell Polyoma Virus' in Cases of Paraffin-Embedded Merkel Cell Carcinoma
EJ Duncavage, JD Pfeifer. Washington University, Saint Louis, MO.

Background: It was recently shown that the majority of cases of Merkel Cell Carcinoma (MCC), a rare and often lethal cutaneous malignancy, harbor a novel, clonally-integrated polyoma virus aptly named Merkel Cell Polyoma Virus (MCPyV). Using both established primers and a novel primer set we studied the prevalence of MCPyV in cases of MCC from routine paraffin-embedded tissue blocks.

Design: We identified 41 cases of MCC in our archives from 1989 to 2008, including 28 cases from unique patients. Of the 41 cases, 20 were primary cutaneous excisions, 17 from metastases, and 4 from recurrences. To ensure similar cellularity and viability across all cases, 2mm representative areas from each tissue block were punched and DNA was extracted following a 48 hour digestion. PCR using two previous published primer sets, LT1 (440bp amplicon) and LT3 (308bp amplicon) as well as a novel primer set MCVPS1 (109bp amplicon) was performed on all samples. Amplification controls including beta globin and a size control ladder were run in tandem. PCR products of the predicted size were detected by 3% agarose gel electrophoresis. Selected PCR products were sequenced to confirm amplicon identity. In addition, the MCVPS1 products were digested with BamH1, yielding an 83bp product that was easily detected by electrophoresis.

Results: A 110bp beta globin control was amplified in all 41 cases. Detection rates of MCPyV for each of the three primer sets was 32 of 41 cases, 78%, (21 of 28 unique cases) for MCVPS1, 17 of 41, 41%, for LT3, and 9 of 41, 22%, for LT1. The variation between primer set detection rates was due to poor DNA quality as supported by low amplification of the higher molecular weight markers in the size control ladder products. All cases that were positive by LT1 and LT3 were positive by MCVPS1.

Conclusions: Previous reports indicate detectable MCPyV in 77% to 80% of MCC cases using the LT1 and LT3 primer sets. We achieved similar findings with a primer set optimized for formalin-fixed tissue that is less prone to the effects of degradation and has the advantage of product verification by restriction fragment length analysis.

---

450 Diagnostic Utility of FISH for $PDGFB$ Locus Rearrangement for the Diagnosis of Dermatofibrosarcoma Protuberans (DFSP)
MR Erickson-Johnson, RS Macarenco, DA Wada, LE Gibson, RV Lloyd, AM Oliveira. Mayo Clinic, Rochester, MN.

Background: Dermatofibrosarcoma protuberans (DFSP) is a superficial low-grade sarcoma genetically characterized by the presence of the chimeric gene *COL1A1-PDGFB*, whose oncogenic activity is susceptible to tyrosine kinase inhibitors, including imatinib mesylate. This fusion gene has been detected only in DFSP and giant cell fibroblastoma (GCF). In this study we tested the sensitivity and specificity of a novel FISH assay for the detection of *PDGFB* locus rearrangement in a series of superficial mesenchymal tumors that commonly simulate the histologic features of DFSP.

Design: One hundred-thirteen samples were evaluated for *PDGFB* locus rearrangement by fluorescence in situ hybridization (FISH) on 4 um thick formalin-fixed paraffin-embedded tissue sections: 32 DFSPs, 16 giant cell fibroblastomas (GCF) (6 pure and 10 mixed GCF/DFSP), 17 cellular fibrous histiocytomas, 10 dermatofibromas, and 12 neurofibromas. We also investigated additional samples from 16 reactive inflammatory fibroblastic tissues, 4 desmoplastic melanomas, 2 myxofibrosarcomas, 2 unclassifiable spindle cell neoplasms, and 2 adenocarcinomas with extensive desmoplasia. Tissues were probed using a custom-designed probe flanking the *PDGFB* locus on chromosome 22q13, and a total of 200 cells were evaluated/sample by 2 technologists without prior knowledge of the diagnosis.

Results: Twenty-nine (of 32) DFSP (91%) showed rearrangement associated with low level copy gains of the *PDGFB* locus. All GCF and mixed GCF/DFSP (16/16) showed unbalanced rearrangement of the *PDGFB* locus. However, copy gains of the *PDGFB* locus were found only in mixed GCF/DFSP. All other tumors and reactive conditions were negative for *PDGFB* rearrangement.

Conclusions: These results indicate that the detection of *PDGFB* locus rearrangements by FISH is sensitive (94%) and specific (100%) for the diagnosis of DFSP, GCF and mixed DFSP/GCF. These results support the diagnostic utility of this assay to discriminate these tumors from tumors that may overlap DFSP/GCF histologically. Furthermore, the identification of *PDGFB* locus rearrangement may be used for therapeutic tailoring, owing to susceptibility of *COL1A1-PDBGB* to small tyrosine kinase inhibitors.

451 Microscopic Imaging of Lymphangiogenesis in Cutaneous Malignant Melanoma: Still a Questionable Predictor of Sentinel Lymph Node Metastasis

G Falconieri, G DeMaglio, D Camilot, S Pizzolitto. General Hospital, Udine, Italy.

Background: Several parameters have been devised to predict sentinel lymph node (SLN) involvement in infiltrating cutaneous malignant melanoma, including tumor thickness, microscopic depth (or Clark level) of invasion, vascular involvement, ulceration, and decreased peri- and/or intratumoral lymphoid infiltration. However, the role of lymphangiogenesis in melanoma is not clear, and specific studies addressing lymphatic vessel density (LVD) and SLN status are underreported.

Design: All cases of invasive melanoma microscopically featuring more than 0.75 mm thickness with available SLN biopsy were retrieved. Paraffin sections from primary tumors were stained with monoclonal antibody D240 (or podoplanin) obtained from a commercial source. Histologic sections were adequate if they had at least 5 microscopic tumor fields for scanning at 20x magnification when using a 25x eyepiece. LVD per square millimeter was assessed by counting lymphatics on at least 5 consecutive tumor fields. Microscopic assessment of extratumoral lymphatic involvement was also carried out.

Results: A total of 136 melanomas fulfilling the design criteria were included in the study. Metastatic SLNs were seen in 29/136 cases (21.3%). In positive SLN cases, LVD in primary melanoma ranged from 0.05 to 1.84 per square millimeter (average 0.34); in negative SLN cases, LVD ranged from 0.05 to 5.1 per square millimeter (average 1.29), P=0.34. Microscopic involvement of peritumoral dermal/hypodermal lymphatics was documented in 7/29 melanomas associated with a positive SLN and in 4/107 cases of negative SLN biopsy (P=0.005).

Conclusions: A low LVD in invasive melanoma is more frequently associated with a positive SLN, although the difference was found to be not statistically significant. Involvement of extratumoral lymphatics proved to be a better predictor of SLN metastases.

452 No Evidence of Epstein-Barr Virus Association with Angioleiomyomas, Pilar Leiomyomas or Cutaneous Leiomyosarcomas in Immunocompetent Individuals

MP Fernandez, TL Davis. University of Texas Health Science Center, San Antonio, TX; South Texas Dermatopathology Laboratory, San Antonio, TX.

Background: Epstein-Barr virus-associated smooth muscle tumors (EBV-SMT) represent a distinct and rare subset of smooth muscle neoplasms occurring in immunocompromised individuals, typically at visceral sites. Some of these tumors demonstrate a close relationship to small vessel walls, suggesting these structures may be the site of origin. Angioleiomyomas are common tumors that arise from the smooth muscle cells of vessel walls, and involve the subcutaneous tissue and dermis.

Design: This study was carried out to assess the potential association of Epstein-Barr virus (EBV) in a spectrum of cutaneous and subcutaneous smooth muscle tumors in immunocompetent individuals. Tissue sections from 20 smooth muscle tumors (12 angioleiomyomas, 3 pilar leiomyomas, 1 cutaneous myopericitoma and 4 primary cutaneous leiomyosarcomas) were studied by in-situ hybridization for EBV-encoded early RNA's (EBER). Each case was also evaluated for the presence of primitive round cell areas and presence of infiltrating lymphocytes, features characteristic of EBV-SMT.

Results: The histopathology of the 20 cutaneous and subcutaneous smooth muscle tumors showed diagnostic features on all cases. All twenty smooth muscle tumors were negative for EBER. Positive and negative controls were satisfactory. Only one case, the cutaneous myopericytoma, showed areas of round cells with a primitive appearance; none of the tumors contained infiltrating lymphocytes.

Conclusions: The absence of EBER in the 20 cases of cutaneous and subcutaneous smooth muscle tumors tested in this study provides further evidence to support to the notion that EBV-SMT arise only in the setting of immunodeficiency.

453 Differentiating Melanoma In Situ from Severely Dysplastic Nevus with Anti-MART-1 Versus Anti-MiTF Immunohistochemistry: The Arkansas Experience

AJ Finn, BR Smoller, KM Hiatt. University of North Carolina Hospitals, Chapel Hill, NC; University of Arkansas for Medical Sciences, Little Rock, AR.

Background: The distinction of melanoma in situ (MIS) from severely dysplastic nevus (SDN) is routinely complicated by coincident keratinocytic atypia and/or prominent interface change. Immunohistochemical stains for the melanoma antigen recognized by T cells (MART-1) can aid in diagnosis by highlighting lentiginous proliferation and pagetoid scatter not otherwise appreciated. However, recent reports of reactivity against nonmelanocytic cells with one widely used clone, as well as the appeal of a non-melanosome-associated, nuclear stain, have prompted a shift from anti-MART-1 to anti-microphthalmia-associated transcription factor (MiTF) antibody at our institution and others.

Design: In order to determine whether this shift was tantamount to a change in diagnostic criteria, we compared the number of diagnoses of MIS to that of SDN on the University Dermatopathology Service for the 11-month periods that directly preceded and followed the introduction of the anti-MiTF stain.

Results: We found the ratio of MIS to SDN diagnoses to be identical during both periods, including in the immunostained group, despite the sustained and near complete transition from anti-MART-1 to anti-MiTF. Interestingly, most cases of MIS and SDN were decided without the aid of an immunostain, though those that did involve one were more likely to be called MIS.

Diagnoses of MIS and SDN before and after adoption of anti-MiTF immunostain

		TOTAL	NO IMMUNO	ANTI-MART-1	ANTI-MITF
2006-2007	RATIO MIS/SDN	64/74	50/70	12/3	
	%MIS	46	42	80	
2007-2008	RATIO MIS/SDN	118/118	95/113		12/4
	% MIS	50	45		75

Conclusions: This data suggests that the hematoxylin and eosin-stained slide remains the primary means of distinguishing MIS from SDN, with immunostains used mainly for confirmation in highly suspicious lesions with obscuring phenomena. These results and pattern of usage suggest that the increasingly common, subjective preference for anti-MiTF in the diagnosis of MIS should not be the basis of speculation regarding prior misdiagnosis of the same.

454 MicroRNA Expression Profiles Differentiate Spitz Nevus from Primary Malignant Melanoma

CI Garady, J Chen, N Zhang, H Feilotter, V Tron. Queen's University, KIngston, ON, Canada.

Background: Spitz nevus remains a difficult histopathologic diagnosis. Recently, microRNA (miRNA) expression has been successfully used to classify tumors into appropriate lineages.

Design: We speculated that miRNA profiles differ in Spitz nevi as compared to melanoma, and thus could be used as a diagnostic aid. To address this, we compared the miRNA expression profiles of 6 classic Spitz nevi and 8 primary melanoma tumors using archival formalin fixed, paraffin embedded (FFPE) tissue. We have previously confirmed the validity of using FFPE tissue to profile miRNAs using an array platform. The Agilent miRNA microarray platform was used to generate miRNA expression profiles.

Results: We found that unsupervised hierarchical clustering clearly separated Spitz nevi from primary melanoma samples. Furthermore, Significance Analysis of Microarray (SAM) was applied to identify differentially expressed miRNA. We found both up-regulated and down-regulated miRNAs in Spitz nevi.

Conclusions: In view of this finding, microRNA profiling of Spitz nevi may prove to have diagnostic applicability. Further studies will be needed to confirm the significance of this initial observation.

455 Beta-Human Papillomaviruses (HPV) Are Common in Vulvar Squamous Cell Carcinomas and Surrounding Skin

A Glazyrin, A Rohwedder, JA Carlson. Albany Medical College, Albany, NY; Bio-Med Molecular Diagnosis, Kalkar, Germany.

Background: Beta (epidermodysplasia verruciformis associated) HPV types are frequently associated with non-melanoma skin cancers. Their role in carcinogenesis has yet to be elucidated. Our objective was to determine the frequency of EV HPV types in vulvar cancers and surrounding skin.

Design: DNA was extracted from 315 paraffin blocks from 70 excisions from 67 women treated for vulvar neoplasia. These blocks consisted of 142 neoplastic, 137 inflammatory, 7 warts, and 29 normal skin specimens. These samples were tested for the presence of HPV DNA utilizing a broad spectrum of degenerate and type specific primers for alpha and beta HPV types. Expression of G1-S cell-cycle regulators p16, p21, p27, p53, cyclin D1 and retinoblastoma was performed by immunohistochemistry and correlated with HPV DNA status.

Results: HPV DNA was detected in 94% (63/67) of all patients and in 73% (23/315) of all samples- beta HPV genotypes in 82% of patients and 52% of all samples, alpha HPV in 80% and 48%, and co-infection with both in 69% and 27%, respectively. Alpha HPV genotypes detected were HPV 6 (7% of all types), 6c, 16 (32%), 18, 33, 52, 53, and 58, and beta HPV consisted of both known genotypes- HPV 5, 8, 12variant, 14d, 17, 20 (5%), 21, 22variant, 23variant, 36, 38 and 47, and twenty one putatively novel HPV genotypes (most common- DL285 19%). Vulvar squamous cell carcinomas (SCC) and adjacent skin samples could be divided into those associated with vulvar intraepithelial neoplasia (VIN)(41% of all samples) and those associated with lichen sclerosis (LS) (55%). As suspected, VIN and associated SCC and adjacent skin samples showed a strong and significant correlation between the presence of high-risk alpha HPV (16, 18, 33, 52 and 58) and a high p16LI (r=0.6, P=0.0001). In this group, HPV 16 was integrated into the host genome in 32%. In LS and associated SCC and adjacent skin samples, HPV 16 was detected in 30%, did not correlate with cell-cycle markers, and was episomal. In contrast, the presence of putatively oncogenic beta HPV (5, 8, 14d, 17, 20, 38, 47) and DL285 significantly correlated with elevated p21 expression in LS and its associated samples (r=0.3, P=0.0001). No correlation was detected between beta-HPV genotypes with G1-S cell markers for VIN and its surrounding skin samples.

Conclusions: Beta HPV genotypes are frequently present in vulvar SCC and its surrounding skin. HPV genotypes segregated into 2 histologic pathways to vulvar SCC: high risk alpha-HPV with VIN-SCC and oncogenic beta-HPV with LS-SCC.

456 Melanocytic Tumors Express Connexin 43 but Not 26, a Immunohistochemical Analysis in Histologic Materials and Potential Significance of the Findings in Melanocytic Oncogenesis

RH Gormley, T Pasha, H Niu, G Acs, X Xu, PJ Zhang. University of Pennsylvania, Philadelphia, PA; H. Lee Moffitt Cancer Center & Research Institute, Tempa.

Background: Connexins (Cx) are major molecular components of gap junctions vital to cell-cell communication which regulates cell proliferation and death. Cx are thought to have tumor suppressor function. However, there is also mounting evidence to suggest that increased expression of some connexins, particularly Cx26, might increase invasive or metastatic properties of the tumor. The exact role of various connexins in melanocytic oncogenesis remains controversial. Our study examined Cx43 and Cx26 in a series of nevi and melanomas (MM) on routine surgical specimen.

Design: Formalin-fixed paraffin-embedded sections of 26 histologically well-characterized melanocytic lesions, 13 primary MM and 13 nevi, were stained with

monoclonal antibody to Cx43 (clone CXN-6, 1:250) and polyclonal to Cx26 (1:100). Immunoreactivity in tumor cells was evaluated semi-quantitatively based on extent (1-100%) and intensity (0-3) of reactivity. A score of 0-300 was generated by the product of the extent and intensity readings in each case. The level of immunoreactivity for nevi vs. MM was then analyzed.
Results: Significantly higher Cx43 immunoreactivity was detected in MM (mean score 242) than in nevi (mean score 111) (p=0.002 Mann-Whitney). Both MM and nevi expressed minimal or entirely absent Cx 26 immunoreactivity. Staining patterns for both Cx26 and Cx43 were generally punctuate and membranous, but some cells showed a granular cytoplasmic pattern.
Conclusions: The finding of minimal or entirely absent Cx26 reactivity in this series was consistent with some previous studies showing absence of Cx26 expression in nevi and MM but not with others demonstrating increased Cx26 staining at sites of tumor invasion. Most notably, however, is the increased Cx43 staining seen in MM and nevi which is in contrast to results from previous studies reporting reduced or absent expression of Cx43 in nevi and MM. The significantly higher Cx43 level in MM when compared to nevi suggests a oncogenic role of Cx43 in melanocytic tumor progression. It is unclear if this discrepancy is due to the different study models used (clinicopathologic study vs more bench research). Nevertheless, our results failed to confirm the previous research finding and call into question established paradigms for the role of Cx43 in melanocytic oncogenesis.

457   Cutaneous Clear Cell Sarcoma: Clinicopathologic, Immunohistochemical and Molecular Analysis of 12 Cases Emphasizing Distinction from Dermal Melanoma
M Hantschke, T Mentzel, E Calonje, AJ Lazar, H Kutzner. Dermatopathology Bodensee, Friedrichshafen, Germany; St. Johns Institute of Dermatology, London, United Kingdom; M.D. Anderson Cancer Centre, Houston, TX.
Background: Clear cell sarcoma (CCS) represents a distinct clinicopathologic entity with characteristic molecular changes arising most frequently in deep soft tissues of the distal lower extremities in young patients. We analyzed a series of cutaneous CCS in order to emphasize its distinction from dermal melanoma.
Design: We examined cases of CCS from our files and evaluated histologic, immunohistochemical and molecular features Only cases confined to the dermis or dermal cases with minimal invasion of superficial subcutis, demonstrating characteristic molecular changes by FISH were included in the study.
Results: Ten patients were female and 2 were male, age ranged from 6 to 74 years (mean: 35 years; median: 25 years). Involved sites included: foot (4), thigh (2), back (2), and single cases involving upper arm, forearm, palm and anterior abdominal wall. Size ranged from 0.4 to 1.7 cm (mean: 0.97 cm; median: 1 cm). In 4 cases the neoplasm was confined to the dermis, and in the remaining cases there was minimal infiltration of superficial subcutis. The variably cellular neoplasms were composed of confluent nests and bands of plump spindled to round cells containing a pale eosinophilic to clear cytoplasm and enlarged, atypical vesicular nuclei with prominent nucleoli. The mitotic rate ranged from 2 to 20 mitoses per 10 high-power fields, and areas of tumor necrosis were present in 2 cases. Multinucleated, wreath-like giant cells were detected in 8 cases, and band-like stromal hyalinisations were common. Immunohistochemically, neoplastic cells stained positively for all melanocytic markers tested (S-100 protein, Melan-A, HMB-45, NKIC-3, MiTF1), whereas cytokeratins, CD34, actin, and desmin were negative in all cases tested. FISH-analysis revealed *EWSR1*-translocation in all 12 cases, and by RT-PCR a *EWSR1-CREB1* and a *EWSR1-Hiat11* fusion product was detected in one case each. Follow-up information available in 9 cases (range from 2 to 63 months, mean: 22.4 months) revealed local recurrence (2 cases) and regional lymph node metastases (3 cases), one patient died of disease.
Conclusions: CCS may arise rarely in the dermis and should be distinguished from dermal melanoma because of different prognosis and treatment options, and from cellular blue nevus, PEComa, cellular dermatofibroma, and cellular neurothekeoma.

458   A Novel Candidate Gene for Promotion of Melanoma Progression
B Horst, K Chernoff, L Bordone, G Brunner, J Celebi. UCLA, LA, CA; Columbia University, NY, NY; Fachklinik Hornheide, Muenster, Germany.
Background: Malignant Melanoma is the most common fatal skin cancer, and shows the fastest rising incidence of all cancers in the US. Current therapy is restricted to surgical excision during early tumor stages, and treatment strategies for advanced disease have not proven significant durable responses. New molecular and genetic targets are being identified and tested in clinical trials. The aim of the current study was to identify novel genes which may play a role in melanoma progression and offer a potential target for regional or systemic tumor therapy.
Design: New molecular genetic techniques allow high resolution genome-wide exploration of DNA copy number and are effective tools in the search for amplification or loss of chromosomal regions. We performed a genome-wide search using BAC CGH and SNP arrays in 63 metastatic melanomas. Overexpression of candidate genes of amplified regions was confirmed by qPCR. Metastatic melanoma cell lines were screened for overexpression of respective loci and selected to assess the impact on invasive capacity of specific downregulation of target genes. Overexpression was confirmed in an independent series of melanocytic lesions, including nevi, primary melanomas as well as melanoma metastases.
Results: We identified distinct amplifications of the 11q13 genomic region in metastatic melanomas. CyclinD1 on 11q13.2 accounted for a subset of these amplifications. Fine mapping delineated a second amplification core. qPCR revealed amplification of a specific locus encoding a critical signal transduction scaffolding protein at the amplicon center. Metastatic melanoma cell lines with overexpression at this locus were subjected to in vitro invasion assays in the presence of small interfering RNAs and showed a significant reduction in invasive capacity. Increased protein expression

could be confirmed in malignant melanomas as compared to melanocytic nevi by immunofluorescent studies in an independent set of melanocytic tumors.
Conclusions: We have identified a novel target gene by genome-wide screening which shows significant upregulation in metastatic melanomas as compared to benign melanocytic lesions. The reduction in invasive capacity by RNA interference is encouraging and warrants in vivo studies to assess for a potential therapeutic target. As mechanisms of resistance to conventional chemotherapy of metastatic melanoma are being investigated, identification of new molecular and genetic targets is a useful means to advance treatment of melanoma.

459   Dermal Analysis of CDKN1B (p27) Is the Most Useful Cell Cycle Regulator for Grading of Atypical Melanocytic Nevi
EA Husain, C Main, L Pozo, A Blanes, SJ Diaz-Cano. Barts and The London Hospital, London, United Kingdom; Homerton University Hospital, London, United Kingdom; University of Malaga School of Medicine, Malaga, Spain; King's College Hospital, London, United Kingdom.
Background: Atypical (dysplastic) melanocytic nevi (AMN) are clinically heterogeneous malignant melanoma (MM) precursors. The value of cell kinetic, cell cycle regulators and microsatellite profile has not been assessed for AMN grading.
Design: We selected 133 lesions, classified into low-grade AMN (92), high-grade AMN (31), and MIS (10), according to standard criteria. Regular melanocytic nevi (15 junctional, 20 compound) and malignant melanomas (15 radial growth phase and 27 vertical growth phase) were used as controls. The microsatellite patterns of TP53, INK4a (p16), p21WAF1, and p27KIP1 were studied by PCR-capillary electrophoresis after topographic microdissection (junctional, superficial and deep dermal) and DNA extraction. The same areas were systematically studied for the expression of Ki-67, p53, p21WAF1, and p27Kip1, and scored by topographic compartments, screening the whole compartment in each case. The results (expressed as percentage of positive cells) were compared using analysis of variance and Student t-test, and considered significant if P<0.05. Results were statistically analyzed regarding grading (low vs. high) and topography (junctional vs. dermal).
Results: A decreasing junctional-dermal marker expression gradient was observed, showing statistically significant differences for TP53, RB1, CDKN2A and CDKN1B at the junction and CDKN1B at the dermis when comparing low-grade and high-grade AMN.

Statistically significant cell cycle regulators for AMN grading

	TP53-Junct	RB1-Junct	CDKN2A-Junct	CDKN1B-Junct	CDKN1B-Derm
Low-grade AMN	2.3±3.1	18.8±17.5	44.4±18.3	28.5±20.0	30.5±18.8
High-Grade AMN	0.9±1.5	8.8±10.3	52.2±18.6	47.5±22.2	48.7±24.5

AMN = Atypical melanocytic nevi, Junct = Junctional, Derm = Dermal
The microsatellite pattern showed coexistent TP53-CDKN2A-CDKN1B microsatellite abnormalities in high-grade AMN, with dermal TP53 and CDKN1B abnormalities. MM showed coexistent microsatellite abnormalities (CDKN2A-CDKN1B), with no topographic gradient and significantly decreased expression.
Conclusions: Although high-grade AMN accumulates junctional TP53-CDKN1A-CDKN1B microsatellite abnormalities, dermal microsatellite abnormalities for TP53 and CDKN1B are the most specific variables for grading AMN.

460   Dermatopathology Fellowship Program Information: As Elusive as the Fellowship
KA Hutchens, M Dahiya. Loyola University Medical Center, Maywood, IL.
Background: Studies have demonstrated that many medical school, resident, and fellowship applicants use the internet as a first means of accessing information about potential training programs. There is no organized match, or shared time-line, for the fellowship application process in dermatopathology. Prospective applicants must research available programs, application and interview dates, as well as length of the program (either one or two years). This study surveyed the potential adequacy of dermatopathology fellowship program websites in aiding the fellowship applicant.
Design: Current program and web addresses were obtained from the Fellowship and Residency Electronic Database (FREIDA) list of graduate medical education programs (under the dermatopathology specialty section). The hyperlink from the database was used to access individual program websites. An average of fifteen minutes was spent per webpage in order to assess ten content features important to the fellowship applicant, including curriculum, program requirements, length of program, and time-line of application process.
Results: 51.8% (28/54) of dermatopathology fellowship programs had functioning web pages accessible via the database hyperlink and, of those, 85.7% (24/28) had a detailed program description. 96.4% (27/28) listed detailed contact information for applicants. 60.7% (17/28) listed applicant requirements but only 35.7% (10/28) had an online application. 57.1% (16/28) outlined a time-line for application acceptance, interview dates, and decision notification. 71.4% (20/28) explained the training curriculum, but, only 57.1% (16/28) displayed the length of training. 32.1% (9//28) of the sites stated the number of applicants accepted. 10.7% (3/28) included such information as the number of specimens and/or patients the trainee would be expected to encounter during fellowship.
Conclusions: There is no streamlined mass application process for dermatopathology fellowships. Fellowship programs should maintain websites with current data and include pertinent program and applicant information to stream-line, and render more transparent, the dermatopathology fellowship applicant process.

461 Expression of Cancer Testis (CT) Antigens in Merkel Cell Carcinoma (MCC)

AA Jungbluth, D Frosina, K Iversen, G Sapgnoli, KJ Busam. Ludwig Institute for Cancer Research New York, New York, NY; University Hospital, Basel, Switzerland; Memorial Sloan-Kettering Cancer Center, New York, NY.

Background: CT antigens such as MAGE, CT7 and NY-ESO-1 have been identified by their ability to elicit B- and T-cell responses in the autologous host. They are expressed in a wide variety of cancers but not in normal adult tissues except testicular germ cells. Based on their immunogenecity and tumor-associated expression pattern, CT antigens are under investigation as vaccine targets for the immunotherapy of cancer. They may also be useful for diagnostic applications in surgical pathology. We previously identified several novel CT antigens and generated monoclonal antibodies (mAbs) for protein expression studies of various CT antigens. MCCs are rare neuroendocrine cutaneous carcinomas. They occur most commonly in older patients, and tend to metastasize early. Except surgical removal of the primary, there is no effective treatment for advanced disease. Hence, MCCs carry a dismal prognosis. Expression of CT antigens has not been analyzed in MCCs albeit their presence may offer additional treatment options and/or could be helpful as diagnostic tool in surgical pathology.

Design: 60 cases of MCC were retrieved from the archives of the Dept. of Pathology of MSKCC. Tissue micro arrays were constructed employing a minimum of 3 representative cores/case. Immunohistochemistry (IHC) was done using the following mAbs (to the following antigens): MA454 (MAGE-A1), M3H67 (MAGE-A3), 57B (MAGE-A4), E978 (NY-ESO-1, CT7-33 (CT7/MAGE-C1), #26 (GAGE, Transduction Labs, Lexington, KY), CT10#5 (CT10/MAGE-C2). Immunoreactivity was graded according to the amount of immunopositive tumor cells as: foc - ~5%; + - 5-25%; ++ 25-50%; ++ - 50-75%; ++++ - >75%.

Results: There was little expression of CT antigens. Most prevalent staining was seen with mAb M3H67 to MAGE-A3. Expression for each mAb was as follows: MA454: 0%, M3H67: 6.7%, 57B: 4.6%, CT7-33: 33:2.6%, CT10#5: 2.5%, E978: 2.2%, #26: 2.6%. Most positive cases showed restricted expression of antigens and only two cases were immunopositive in more than 75% of the tumor.

Conclusions: Though other skin cancers such as melanoma are among the tumors with the most prevalent expression, CT antigens are poorly expressed in MCC. Moreover, the few CT antigen positive cases show a very restricted expression pattern within the lesion. We conclude that CT antigens are neither useful diagnostic markers nor useful vaccine targets in Merkel Cell Carcinoma.

462 Percentage of Sentinel Lymph Node Involvement by Metastatic Melanoma as Measured by ACIS Cytometric Image Analysis Is Associated with Survival

S Lauer, R Yaar, A Page, A Hestley, K Delman, G Carlson, C Cohen. Emory University Hospital, Atlanta, GA.

Background: Sentinel lymph node (SLN) biopsy is a common procedure for staging patients with melanoma. Immunohistochemistry for MelanA and HMB45 facilitates examination of SLNs by highlighting small metastases. Previous studies suggest that increased volume of metastatic melanoma in SLNs may be a prognostic factor associated with adverse outcomes. Cytometric image analysis with the ACIS system may be useful for quantitating the amount of melanoma metastasis in SLNs. We aim to quantitate the percentage of SLN involvement by metastatic melanoma using the ACIS system, and to identify a relationship between the %SLN involvement, survival and recurrence.

Design: MelanA and HMB45 stained sections of SLNs from 119 patients with melanoma and a single positive SLN were reviewed, scanned and analyzed using the ACIS digital imaging system. The %SLN involvement was calculated by dividing the area staining positively for MelanA and HMB45 by the total lymph node area. The %SLN involvement was compared to clinical data for survival, recurrence, Breslow depth, and ulceration.

Results: Metastases stained positively for MelanA and HMB45 in 99.2% and 96.6% of cases. At a mean clinical follow-up time of 82 months, there were a total of 41 recurrences (39%) and 34 deaths (32.4%). Using HMB45 immunostaining, >5% SLN involvement was significantly associated with decreased survival (59.3% vs 77.8%, p=.047). Increased risk of recurrence approached significance (47.5% vs 28.9%, p=.055). Using MelanA staining, >10% SLN involvement was significantly associated with decreased survival (47.8% vs 72.1%, p=.03), while increased risk of recurrence approached significance (56.5% vs 36.0%, p=.07). No difference in survival or recurrence was identified when using a cutoff of >10% for HMB45 and >5% for MelanA. The %SLN involvement was not associated with Breslow depth or ulceration. A head and neck primary site was associated with a higher %SLN involvement compared to all anatomic sites (22.3% vs 12.51%, p=0.02).

Conclusions: Increased %SLN involvement by metastatic melanoma as measured by ACIS image cytometry of HMB45 and MelanA staining is significantly associated with decreased survival. Increased risk of recurrence also approached significance with higher percentages of SLN involvement. These findings suggest that %SLN involvement may be a useful prognostic parameter in melanoma patients with single positive SLN metastases.

463 Detection of Merkel Cell Polyomavirus in Merkel Cell Carcinoma, Small Cell Carcinoma of the Lung, and Other Skin Cancers

KL Lee, S Husain, MM Mansukhani. Columbia University Medical Center, New York, NY.

Background: Merkel cell carcinoma (MCC) is a rare yet aggressive skin cancer in humans that tends to occur in elderly and immunosuppressed patients. A recent study discovered an association between MCC and a new human polyomavirus, Merkel cell polyomavirus (MCPyV).

Design: Our study looks for MCPyV by PCR in formalin-fixed, paraffin-embedded tissue from 25 MCC, other skin cancers—10 squamous cell carcinoma (SCC), 10 basal cell carcinoma (BCC), 8 melanoma—and 6 small cell carcinomas of the lung. Additionally, control tissue was analyzed from 9 cases of various inflammatory skin conditions. Two primer-probe sets directed at the VP1 gene and large T antigen gene of MCPyV were utilized for real-time PCR detection of viral DNA.

Results: MCPyV was detected in 52% of MCC (13/25), while no MCPyV was found in the other skin cancers (0/10 SCC; 0/10 BCC; 0/8 melanoma) nor in the small cell carcinomas of the lung (0/6). None of the inflammatory skin cases (0/9) were positive.

Conclusions: In this study, MCPyV was identified in over half of MCC cases, but was not detected in other skin cancers, small cell carcinoma of the lung, or control skin samples.

464 Immunohistochemical Techniques To Differentiate Primary Versus Metastatic Mucinous Carcinoma in the Skin

G Levy, A Finkelstein, J McNiff. Yale New Haven Hospital, New Haven, CT.

Background: Mucinous carcinoma is a rare entity that can occur in the skin as a primary cutaneous malignancy or as a metastasis, typically from breast or colon.Metastatic and primary cutaneous mucinous carcinomas are morphologically identical.There are reports that staining with antibodies to p63, D240, CK 5/6, and CD15 is helpful in distinguishing primary and metastatic adenocarcinomas in the skin.Few studies, however, have evaluated staining patterns specifically of mucinous carcinomas in the skin.We applied this immunohistochemical panel to primary mucinous carcinomas of the skin, breast and colon, and metastatic mucinous carcinomas to the skin, in an attempt to identify patterns of staining to differentiate between these entities.

Design: Five cases of primary mucinous carcinoma of the skin, breast, and colon were identified in the files of the Departments of Surgical Pathology and Dermatology. Additionally, two cases of metastatic mucinous breast carcinoma to the skin were also identified. These cases were stained with antibodies to p63, CD15, CK5/6, D2-40, CK7, and CK20. The staining pattern of primary cutaneous mucinous carcinoma was compared to staining of mucinous carcinoma metastatic to skin, and primary mucinous carcinoma of breast and colon.

Results: All cases of primary mucinous carcinoma of skin were positive for CK7. Only 40% labeled with antibodies to p63, and all were negative for CD15, D2-40, CK20, and calponin. The breast mucinous carcinomas metastatic to the skin were negative for all markers except CK7. The primary breast carcinomas were all positive for CK7, and negative for calponin, CK20, D240, CK5/6, and CD15. Staining for p63 was identified in 60% of cases of breast mucinous carcinoma. The primary mucinous colonic carcinomas were negative for all markers except CK20.

Conclusions: Unlike other primary adenocarcinomas of the skin, which can often be differentiated from metastases by positive staining for CK 5/6, D2-40 and P63, mucinous carcinomas of the skin are typically negative for these markers. In a small subset of cases (20% in this series), positive labeling for CK5/6 in primary mucinous carcinoma of skin may help establish a definitive diagnosis. Contrary to previous published reports, immunohistochemical stains for myoepithelial cells were not helpful in differentiating primary from metastatic lesions in our series. Labeling for CK7 and CK20 is helpful in differentiating colon carcinoma from breast or skin malignancies, but does not differentiate primary skin lesions from breast metastases to skin.

465 BD ProEx™ C Immunostaining in Cutaneous Melanocytic Lesions

M Li, D Frishberg, AE Walts, S Bose. Cedars-Sinai Medical Center, Los Angeles, CA.

Background: ProEx C is a novel immunohistochemical marker combining antibodies against topoisomerase IIa and minichromosome maintenance protein 2 intended to detect cells with aberrant S-phase induction. Recently we reported expression of ProEx C in perineal melanomas. The purpose of our study is to evaluate the expression of ProEx C in malignant melanomas (MM), dysplastic nevi (DN) and intradermal melanocytic nevi (IDMN).

Design: Thirty cases (ten each of MM, DN and IDMN) were retrieved from our files. After H&E stained slides were reviewed and diagnoses confirmed, ProEx C and Ki-67 immunostains were performed on serial sections of a representative formalin fixed paraffin embedded block from each case with appropriate controls. Immunostains were reviewed and percent positivity recorded. Staining in ≤5% of lesional cells was scored as negative.

Results: Positive staining for ProEx C was seen in 7/10 (70%) of the MM (including 6/6 vertical growth phase MM and 1/3 radial growth phase MM) and 1/10 (10%) of the DN tested. Strong ProEx C positivity was observed in ≥15% of lesional cells in all of the positive staining MM. The one positive DN showed ProEx C staining in 10% of lesional cells. All 10 (100%) of the IDMN, 9/10 (90%) of the DN, and 3/10 (30%) of the MM (comprising 2/3 radial growth phase MM and 1/1 indeterminant growth phase MM) stained negative. In each case studied, ProEx C and Ki-67 staining was similar in pattern and distribution. In cases with ≤5% positivity, staining was largely confined to the junctional component. In cases with >5% positivity, staining was randomly distributed throughout the lesion.

Conclusions: Our findings suggest that a) Melanocytic lesions show differential expression with ProEx C. Most MM and one DN studied stained positive while all IDMN stained negative. b) ProEx C positivity correlates with growth phase in MM. Positive staining in ≥15% of lesional cells is strongly associated with vertical growth phase. c) ProEx C and Ki-67 show similar staining patterns in cutaneous melanocytic lesions. The potential of ProEx C immunostaining alone or in combination with Ki-67 to help stratify histologically similar cutaneous melanocytic lesions into prognostically different subgroups merits further study.

466   Matrix Metalloproteinase-9 (MMP-9) and Vascular Endothelial Growth Factor (VEGF) Are Regulated by Histone Lysine Specific Demethylase 2 (LSD2) in Cultured Human Melanoma Cells
C Lian, B Lian, M-Y Hsu, Y Shi, B Woda, A Deng, R Han. University of Massachusetts, Worcester, MA; Brigham & Women's Hospital, Harvard Medical School, Boston; Brigham & Women's Hospital, Harvard Medical School, Boston, MA.
Background: Matrix metalloproteinases (MMPs) and vascular endothelial growth factors (VEGFs) are involved in tumor invasion, metastasis and angiogenesis, and have been implicated as progression markers in melanoma. The molecular mechanisms that regulate the gene transcription of MMPs and VEGFs in melanoma are unknown. Histone modification is a key mechanism in epigenetic regulation of gene transcription, which is recently recognized as a crucial player in various physiological and pathological processes.
Design: Here we investigated the role the newly discovered lysine specific demethylase 2 (LSD2), a key enzyme in epigenetic regulation, in regulating both MMPs and VEGFs in melanoma by using cultured human melanoma cell line WM793. Knockdown of LSD2 expression was achieved by an adeno-associated virus (AAV) based siRNA delivery system. Both MMP-9 and VEGF mRNA expression was measured by quantitative real-time RT-PCR.
Results: LSD2 AAV siRNA effectively knocked down LSD2 gene transcription in cultured human melanoma cell line WM793. Both MMP-9 and VEGF mRNA expression was significantly down-regulated following LSD knockdown.
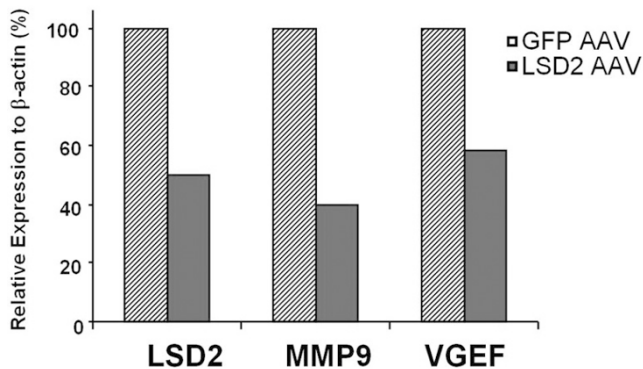
Conclusions: These findings suggest that malignant phenotypical changes associated with tumor invasion, metastasis and angiogenesis is associated with epigenetic alterations mediated by histone modification by LSD2.

467   Correlation of Microphthalmia Associated Transcription Factor (MITF) Protein and Melastatin (MLSN) mRNA Expression in Melanocytes
S Lu, SE Yang, JS Ross, CE Sheehan, A Slominski, JA Carlson. Albany Medical College, Albany, NY; University of Tennessee HSC, Memphis, TN.
Background: Melastatin (MLSN; a.k.a. TRPM1) is suspected to regulate melanocyte differentiation and proliferation. Its expression is regulated by the essential melanocyte transcription factor MITF (microphthalmia-associated transcription factor). In melanoma progression, MITF expression is preserved while MLSN mRNA expression is lost-presumably conferring a less differentiated state and more aggressive tumor phenotype. In this study, we examined the correlation of MLSN mRNA expression with MITF in melanocytes from normal skin, scars, hair follicles and melanocytic nevi.
Design: Samples of 100 normal skin, 8 scars, and 10 congenital and neurotized melaocytic nevi were evaluated for MLSN mRNA transcription as detected by chromogenic in situ hybridization (CISH). Expression was measured per one hundred basal keratinocytes (labeling index (LI)) and compared to MITF expression detected by immunohistochemistry.
Results: In paired normal samples, intraepidermal melanocyte expression of MLSN mRNA strongly correlated with MITF expression (r=0.5, p=0.0001), with LI of 10±0.5 and 12±0.5, respectively. In follicular bulbs and infundibula, lower, but similar LIs were identified: 5±3 vs. 9±6 / 7±4 vs. 9±3, respectively. In the isthmic-follicular bulge region, MITF, not MLSN expression was identified. In scars, MLSN expression decreased relative to MITF with LI of 6±1 and 12±2. The differential expression between MITF and MLSN was significantly greater for melanocytes in scars than normal (6±2 vs. 2±0.5, P=0.002). In congenital melanocytic and neurotized nevi, the intensity of MITF and MLSN expression decreased with melanocyte descent into the dermis. Deep dermal type B and type C melanocytes exhibiting faint or no MITF or MLSN mRNA signal.
Conclusions: Loss of MLSN mRNA expression relative to MITF was associated with regenerative (melanoblast) phenotype overlying scars and 'melanocyte maturation' to type C or neurotized melanocytes in melanocytic nevi. These results support the contention that MLSN mRNA expression is a marker of a fully differentiated melanocyte.

468   Diagnostic Value of CD33 by Immunohistochemistry in Leukemia Cutis
L Ma, DSL Kim, J Cutlan, C Ross, M Lim, D Fullen. University of Michigan, Ann Arbor, MI.
Background: CD33 is a glycosylated transmembrane protein that is expressed in committed myeloid precursor cells. It is down-regulated in mature granulocytes, but is maintained in monocytes/macrophages. CD33 is an important marker in immunophenotyping acute leukemias. However, the evaluation of CD33 expression has previously been restricted to flow cytometric (FC) analysis of fresh cell preparations. Recently, a new monoclonal CD33 antibody was found to react in paraffin-embedded

bone marrow samples with results comparable to FC analysis. In this study, we sought to investigate the diagnostic utility of CD33 by immunohistochemistry (IHC) in cutaneous leukemic infiltrate.
Design: CD33 (clone PWS44) IHC stain was performed on formalin-fixed and paraffin-embedded skin specimens, including 23 cases of leukemia cutis (1 ALL, 7 AML-M1-3, 8 AML-M4-5, 1 AML-M6, and 6 AML-Nos) and 4 cases of inflammatory skin diseases. Twenty cases had FC data available. A cytoplasmic stain in greater than 10% of the tumor cells was considered positive. The staining was scored by two pathologists based on the percentage of immunoreactive cells (1+ = 10-50%; 2+ = >50%) and intensity (weak vs. moderate/strong).
Results: In normal skin and inflammatory skin diseases, CD33 reacted with macrophages/histiocytes. In lesions of leukemia cutis, CD33 was detected in 18 of 23 cases, with the majority (16/18, 89%) showing diffuse and moderate to strong reactivity. Sixteen of these positive cases had FC data available and the FC data correlated well with the IHC results. The two cases with weak IHC staining also had dim immunofluorescence seen with FC. Four of 5 negative cases demonstrated CD33 negativity by FC while one case had no FC data.

Result Summary				
	Positive cases	IHC+/FC+	Negative cases	IHC-/FC-
AML, Nos	5/6	5	1/6	1
AML, M1-3	6/7	4*	1/7	1
AML, M4-5	6/8	6	2/8	1**
AML, M6	1/1	1	0/1	0
ALL	0/1	0	1/1	1
Total	18/23	16	5/23	4

*2 cases had no FC data; **1 case had no FC data
Conclusions: CD33 monoclonal antibody labels the majority of cutaneous lesions of acute myeloid and monocytic leukemia. There is an excellent concordance between CD33 IHC results on skin acute leukemia lesions and the patient's FC data. Therefore, CD33 would be a useful diagnostic marker in evaluating cutaneous leukemic infiltrate.

469   The Expression of mTOR Pathway Proteins in Cutaneous Lymphomas
L Ma, PN Bogner, S Tripp, SL Perkin, D Abbott, M Lim. University of Michigan, Ann Arbor, MI; University of Utah, Salt Lake City, UT; Ohio State University, Columbus, OH.
Background: Mammalian target of rapamycin (mTOR) is a protein kinase that regulates cell growth. The translation regulators p70S6 kinase (p70) and pS6 ribosomal protein (pS6) are well characterized downstream effectors of the mTOR pathway. Previous studies showed that mTOR pathway proteins are up-regulated in some systemic anaplastic large cell lymphomas (ALCL) and systemic B-cell lymphomas. In this study, we examined the expression of mTOR pathway proteins in primary cutaneous lymphomas.
Design: Using tissue microarrays, immunostaining of mTOR pathway proteins (phospho-mTOR, phospho-p70 and phospho-pS6) was performed on a total of 74 lymphoid lesions, including 6 cutaneous lymphoid hyperplasias, 7 cutaneous ALCLs, 4 systemic ALCLs, 11 mycosis fungoides (MF), 15 lymphomatoid papulosis (LyP), 10 MF with large cell transformation (MF-LCT), 11 primary cutaneous B-cell lymphomas (PCBCL) and 10 systemic B-cell lymphomas with secondary skin involvement (SBCL). A marker was considered positive if >10% of lesional cells showed nuclear and/or cytoplasmic staining.
Results: In cutaneous lymphoid hyperplasia, p70 and pS6 stained reactive B-cells, while mTOR was negative. Subsets of systemic and cutaneous ALCL stained positive for mTOR (weak), p70 and pS6 (moderate to strong). mTOR, p70 and pS6 reactivity was detected in some cases of LyP, MF, and MF-LCT. For cutaneous B-cell lymphomas, both PCBCL and SBCL expressed mTOR, p70 and pS6 at comparable levels. Results are summarized in Table 1.

Table 1			Overall Positivity	
Diagnoses	Total cases	mTOR	p70	pS6
Systemic ALCL	4	2/4 (50%)	3/4 (75%)	1/4 (25%)
Cutaneous ALCL	7	1/7 (14%)	3/7 (43%)	2/7 (29%)
LyP	15	5/15 (33%)	4/15 (27%)	8/15 (53%)
MF	11	5/11 (45%)	2/11 (18%)	4/11 (36%)
MF-LCT	10	4/10 (40%)	4/10 (40%)	6/10 (60%)
Cutaneous lymphoid hyperplasia	6	0/6 (0%)	3/6 (50%)	4/6 (67%)
Cutaneous. B-cell lymphoma	11	6/11 (55%)	4/11 (36%)	5/11 (45%)
Systemic B-cell lymphoma	10	6/10 (60%)	4/10 (40%)	2/10 (20%)

Conclusions: 1. Compared to benign cutaneous lymphoid hyperplasias, mTOR levels are elevated in primary cutaneous T-cell lymphoproliferative disorders and mTOR pathway proteins are upregulated in PCBCL and SBCL. 2. p70 and pS6 are activated in MF-LCT, probably through upstream proteins other than mTOR. 3. The activation of mTOR pathway proteins in cutaneous lymphoma suggests potential for Rapamycin as a therapeutic agent.

470   Long Term Follow-Up in Patients with Pigmented Epithelioid Melanocytoma
RV Mandal, R Murali, KF Lundquist, BD Ragsdale, PJ Heenan, SW McCarthy, MJ Mihm, RA Scolyer, A Zembowicz. Massachusetts General Hospital, Boston, MA; Royal Prince Alfred Hospital, Camperdown, NSW, Australia; Central Coast Pathology, San Luis Obispo, CA; Cutaneous Pathology, Nedlands, Western Australia, Australia; Lahey Clinic, Burlington, MA; DermatopathologyConsultations.com, Belmont, MA.
Background: Pigmented epithelioid melanocytoma (PEM) is a recently defined entity encompassing epithelioid blue nevus of Carney complex and some tumors previously considered as a so-called animal-type melanoma. Loss of the Carney complex gene, protein kinase regulatory subunit R1α is observed in the majority of sporadic and

Carney complex-associated PEMs. PEMs frequently metastasize to lymph nodes, and yet the initial average 2 year follow-up suggested a more favorable outcome than for conventional melanomas.

Design: In this report, we detail long-term follow up of 28 patients from North America and Australia with PEM.

Results: The patient's median age was 21 years, with 9 males and 16 females. Nine of the patients developed sentinel node metastases. After a median of 67 months of follow-up (range 39 to 216 months), all patients are alive and free of disease.

Conclusions: These findings provide further evidence that PEM is a unique low-grade melanocytic tumor with limited metastatic potential (to lymph nodes), but an indolent long-term clinical course.

471 Atypical Fibroxanthoma (AFX): Clinicopathologic Characteristics and Natural History in a Large Single-Institution Series

TW McCardle, JS Zager, M Bui, S Shah, A Patel, VK Sondak, JL Messina. H. Lee Moffitt Cancer Center and Research Institute, Tampa, FL; University of South Florida College of Medicine, Tampa, FL.

Background: AFX is a cutaneous sarcoma of probable fibrohistiocytic origin related to pleomorphic sarcoma (malignant fibrous histiocytoma). The typical presentation is a rapidly growing nodule on sun-exposed skin of the elderly, & complete excision is considered curative in most cases. While its behavior is generally low-grade, there is controversy regarding diagnostic criteria, optimal surgical tx, adjuvant tx, & the natural history of the dz. We herein present a large single-institution series of AFX, including clinicopathologic characteristics & outcomes, stratified by tx type.

Design: An IRB-approved, retrospective review of the electronic medical record, pathology database, & cancer registry was performed on all pts dx'ed w/ AFX & tx'ed at our institution from (1990-2008). Demographics, tumor size, location, immunostains used, surgery type including excision size & margins, adjuvant tx, & outcomes were compiled.

Results: 47 pts w/ AFX were analyzed, 34 M & 13 F. Median age 74.0 yrs(38-92). Locations included: H&N(40), extremities(4), & trunk(3). Median tumor size was 1.8 cm(0.2-6.0 cm). Vimentin was positive in 16/17(94.1%), CD68 in 24/26(92.3%) & CD10 in 7/7(100%) cases. W/a median f/u interval of 13.5 mos., 8 (17%) pts recurred w/a median time to recurrence of 33.4 mos. 40 pts were tx'ed w/ wide excision (WE), 4 pts w/ Mohs surgery, 1 pt w/ Mohs & WE, 1 pt w/ radiotherapy (XRT); 1 pt had no further tx. Median width of excision was 3.2cm(0.6–7.0cm), w/ a median margin of excision of 1.6cm. 39 pts had negative margins; 7(17.9%) pts were tx'ed w/ XRT, of these 1(14.3%) recurred. 6/39(15.4%) pts w/ negative margins & no XRT recurred. 8 pts had positive margins; 2 received XRT & did not recur. 6 received no further tx, & 2(33%) recurred. Irrespective of margin status, 1/9(11.1%) pts tx'ed w/ XRT recurred, while 7/38(18.4%) pts not receiving XRT recurred. 9(19%) pts died w/ a median time to death of 36 mo's; 1 of these was confirmed to be due to AFX. One case had metastatic dz.

Conclusions: AFX occurs in elderly individuals, predominantly on the H&N. Pts w/ positive margins recurred more often compared to negative surgical margins. However, the risk is reduced w/ XRT. A subpopulation of recurrent tumors may behave in a more aggressive fashion. The mortality rate is low in AFX, but this biased due to its elderly population.

472 Diagnostic Utility of IMP3 in Segregating Metastatic Malignant Melanomas from Benign Nevi in Lymph Nodes

MJ Mentrikoski, L Ma, JG Pryor, LA McMahon, BO Spaulding, GA Scott, HL Wang, H Xu. University of Rochester Medical Center, Rochester; University of Michigan Medical Center, Ann Arbor; Dako North America, Carpinteria; Cedars-Sinai Medical Center, Los Angeles.

Background: Benign melanocytic nevi are encountered within the capsule and trabeculae of lymph nodes. These benign nevi may create diagnostic problems when found within sentinel lymph nodes of patients with cutaneous melanoma. It has previously been shown that insulin-like growth factor-II messenger RNA (mRNA)-binding protein 3 (IMP3), also known as K homology domain-containing protein overexpressed in cancer (KOC) and L523S, has diagnostic value in distinguishing cutaneous melanoma from benign nevi, and that IMP3 is a progression biomarker of malignant melanoma. The aim of this study was to determine if detection of IMP3 expression can be used to segregate metastatic melanoma from benign nevi in sentinel lymph nodes.

Design: Using monoclonal antibodies against IMP3 and Melan-A, 24 sentinel and 5 non-sentinel lymph nodes from 28 patients with metastatic malignant melanoma and 10 sentinel lymph nodes with benign nevi from 9 patients with cutaneous malignant melanoma were examined. Benign nevi were located both in the capsule (n=8) and trabeculae (n=2). Nevic cells were highlighted on Melan-A stained slides, and a diagnosis of melanoma was based on cytologic atypia and comparison with the primary melanomas. Care was taken so that cells positive for Melan-A were the same cells examined when evaluating for IMP3 expression. IMP3 is known to be expressed in lymph node germinal centers, and this was also taken into account. A case was considered positive if more than 10% of the cells of interest showed cytoplasmic IMP3 staining. The staining intensity was graded as weak, moderate, and strong.

Results: Twenty of 29 (69%) sentinel and non-sentinel lymph nodes with metastatic melanoma were immunohistochemically positive for IMP3 with more than 10% of tumor cells stained. The staining intensity was variable from weak to strong. No IMP3 expression was detected in any of benign nodal nevi, while they were highlighted on Melan-A staining. Benign germinal centers were highlighted with IMP3 staining in all cases, which were used as internal positive controls.

Conclusions: A large proportion of nodal metastatic melanomas express IMP3, but benign nodal nevi do not. These findings indicate that IMP3 is a valuable diagnostic biomarker in distinguishing benign nevi from metastatic melanomas in lymph nodes.

473 Dermatomyofibroma: Clinicopathologic and Immunohistochemical Analysis of 56 Cases and Reappraisal of a Rare and Distinct Cutaneous Neoplasm

T Mentzel, H Kutzner. Dermatopathologie Bodensee, Friedrichshafen, Germany.

Background: Dermatomyofibroma represents a rare and distinct benign cutaneous mesenchymal neoplasm of fibroblastic/myofibroblastic differentiation. A large series has been analyzed to further characterize the clinicopathologic spectrum of this entity.

Design: We examined 56 cases of dermatomyofibroma from our routine and referral files to evaluate histologic features. Immunohistochemistry was performed and clinical follow-up was obtained.

Results: 40 patients were female and 8 were male (gender was unknown in 8 cases). Patients age ranged from 3 to 51 years (mean: 30.85 years; median: 30 years). 6 patients were younger than 16 years, and in this age group 3 male and 3 female patients were noted. Neoplasms arose on the shoulder (28%), the upper arm (15%), the neck (13%), the thigh (13%), the chest wall (9%), the back (6%), the axillary fold (4%), and the abdominal wall (4%), and one case each on the forearm, the buttock, and the popliteal fossa. 1 patient presented with two lesions arising simultaneously on both shoulders. Histologically, ill-defined, plaque-like, dermal neoplasms of varying cellularity composed of bland spindled tumor cells were seen in all cases. An infiltration of superficial parts of the subcutis was seen in 23 cases, and in 6 cases deeper parts of the subcutis were involved. Tumor cells contained an ill-defined, pale eosinophilic cytoplasm and fusiform nuclei that were either elongated with tapering edges containing an evenly distributed chromatin or vesicular with small nucleoli and indentations. No significant atypia and no increased proliferativ activity was noted. Tumor cells were set in a collagenous stroma, and in most cases an increased number of elastic fibres was seen. Immunohistochemically, 31 out of 48 cases tested stained at least focally positive for actin, and a focal expression of CD34 was seen in 10 out of 45 cases. The remaining antibodies (S-100, desmin, h-caldesmon, EMA, HHV-8, Factor 13a) were negative. Follow-up information was available in 38 cases (range from 3 to 156 months), and despite marginal or incomplete excision in 17 cases none of the cases recurred or showed progression.

Conclusions: Dermatomyofibroma represents an entirely benign fibroblastic/myofibroblastic dermal neoplasm, arises often but not exclusively in the shoulder and upper arm regions of young females, and has to be distinguished from DFSP, smooth muscle tumors, neurofibroma, desmoplastic spindle cell nevus, perineurioma, cutaneous myofibroma, fibrous hamartoma of infancy, and connective tissue nevus.

474 Quantitative Evaluation of Activated Cytotoxic Lymphocytes in Melanocytic Lesions Using Laser Confocal Microscopy

EC Miller, L Ang, M Dahiya, SR Tahan. Beth Israel Deaconess Medical Center, Boston, MA; Loyola University Medical Center, Chicago, IL; Harvard Medical School, Boston, MA.

Background: The histologic features of regression in melanocytic lesions can be difficult to differentiate from effect of prior trauma, regression, and tumor infiltrating lymphocytes (TILs). Previous studies have shown that T-cells play an important role in these conditions. We utilized a novel application of laser confocal microscopy to investigate possible differences among these lesions in proportion of activated CD8+ lymphocytes as measured by expression of TIA-1.

Design: Cases of melanoma with regression (n=12), melanoma with TILs (n=15), halo nevi (n=8), dysplastic nevi with prior biopsy (n=9), and benign nevi (BN) with prior biopsy (n=6), from the pathology archives were studied. Paraffin blocks were sectioned at 4 microns, incubated with primary antibodies to CD8 and TIA-1, followed by incubation with fluorescein (CD8) and CY5 (TIA-1) conjugated secondary antibodies. Confocal images were obtained using Zeiss LSM510 confocal system (20x/0.8 objective). All CD8+ (green) cells co-expressing TIA-1 (red) cells were counted and divided by total CD8+ population for each case. Group means were compared using the unpaired student T-test.

Results: The mean % of TIA-1+CD8+ cells for each group is displayed.

%TIA-1+/CD8+ cells by group

	BN with bx	DysN with bx	Halo nevus	Mel TILs	Mel w regression
# cases	6	9	8	15	12
%TIA+CD8+ (mean)	85.8	89.4	92.3	87.5	89.0

The highest percentage of TIA-1+ CD8+ cells was found in halo nevi. Unpaired means comparison revealed a significant difference in the percentage of activated CD8+ lymphocytes in biopsy sites within banal nevi versus halo nevi (85.8 vs. 92.3, P=0.03) and halo nevi versus melanoma with TILs (92.3 vs. 87.5, P=0.05).

Conclusions: This study demonstrates the novel application of laser confocal microscopy to quantitate in paraffin sections the proportion of lymphocytes with specific phenotype. The highest proportion of activated cytotoxic T-cells was found in halo nevi, exceeding that of biopsy sites within nevi and tumor infiltrating lymphocytes of melanoma. No difference was, however, found between the population of lymphocytes in melanomas with regression and tumor infiltrating lymphocytes or between melanomas with regression and biopsy sites in melanocytic nevi. This analysis does not reveal distinguishing differences among these groups, however additional studies of other activated lymphocyte populations are underway.

475 Prognostic Significance of CCR10 and CCL27 Expression in Primary and Metastatic Cutaneous Malignant Melanoma

C Monteagudo, D Ramos, A Pellin-Carcelen, JA Lopez-Guerrero, V Alonso, E Jorda, A Pellin. University of Valencia, Valencia, Spain; Fundacion Instituto Valenciano de Oncologia, Valencia, Spain; Hospital Clinico Universitario, Valencia, Spain.

Background: A role for the CCR10 chemokine receptor in cutaneous melanoma metastasis was originally proposed due to the fact that its ligand, CCL27, is expressed in the epidermis. However, recent data suggest a role for CCR10 and CCL27 in immune escape of tumor cells leading to tumor progression.

Design: Our goal was to evaluate, by Real-Time Quantitative PCR, mRNA expression of CCR10 and its ligand, CCL27, in primary and metastatic human cutaneous malignant melanomas. Expression was evaluated in 88 frozen tumor samples: 41 primary melanomas [18 thin (≤1 mm); 23 thick (>1mm)] and 47 melanoma metastases (18 "in transit" metastases, 16 lymph node metastases, and 13 distant metastases). Expression in primary melanomas was correlated with prognostic clinicopathologic factors and clinical follow-up. In order to evaluate the cell types responsible for chemokine ligand and receptor expression, an immunohistochemical study (avidin-biotin immunoperoxidase) was also performed in adjacent frozen sections.

Results: CCR10 mRNA expression was significantly higher in primary melanomas which subsequently developed lymph node metastasis (p=0,026), and in primary tumors with >1 mitosis/mm² (p=0,033). Unlike the situation in thin melanomas, CCR10 levels were higher in thick tumors than in metastases (p=0,013). CCL27 expression was higher in primary tumors than in metastases (p=0,000). CCL27 immunoreactivity was found in basal and suprabasal epidermal cells and in some tumor cells. CCR10 immunostaining was present in most tumor cells.

Conclusions: Up-regulation of CCR10 expression in primary melanomas is associated with further development of lymph node metastases but not cutaneous in transit or distant metastases. Therefore, CCR10 may serve as a selective prognostic marker in the management of melanoma patients. In contrast, down-regulation of CCL27 in melanoma metastases supports the proposed role of this chemokine in antitumor immune response, but the absence of differences in expression among primary tumors limits its predictive value. *Performed with FIS PI07/1203 grant, from Fondo de Investigación Sanitaria, Spain.*

476 Expression of Ki-67 in Benign, Atypical, and Malignant Hidradenomas

RM Nazarian, P Kapur, A Piris, MC Mihm, MP Hoang. Massachusetts General Hospital, Boston, MA; UT Southwestern Medical Center, Dallas, TX.

Background: The histologic features of an atypical hidradenoma are worrisome for an increased risk of recurrence and possible malignant potential; however, prior studies with immunohistochemistry or follow-up have not been reported. In addition, immunohistochemical analysis of hidradenocarcinoma exists in the literature mainly as case reports and a single series of six cases.

Design: Archival materials were retrieved from the MGH pathology (1978-2008) and MCM consultation files (2000-2006). The slides were reviewed by MPH and MCM and the following features were graded as either present or absent: loss of circumscription, infiltrative growth pattern, deep extension, necrosis, perineural invasion, vascular invasion, nuclear pleomorphism, and greater than 4 mitoses per 10 high-power fields. Tumors with ≥ 3, 1 or 2, and none of the cited features were classified as malignant, atypical, and benign hidradenoma, respectively. Eight metastasizing adnexal carcinomas were included as the control group. Percentage of Ki-67 immunoreactivity was scored and averaged for 5 HPFs (~500 cells per field) independently by RMN and MPH. The mean Ki-67 scores of the different groups were compared using Mann-Whitney U non-parametric tests.

Results: A statistically significant difference (two-tailed p value of < 0.05) in mean Ki-67 expression was observed between group #1 vs #2 (p=0.045), #1 vs #3 (<0.001), #1 vs #4 (0.002), #2 vs #3 (<0.001), #2 vs #4 (0.002) (see table 1). Follow-up was available for 6 hidradenocarcinomas (range: 2 months to 2 years; median: 11 months) and showed no evidence of disease. Follow-up was available for 11 atypical hidradenomas (range: 6 months to 16 years; median: 2 years) and showed no recurrences.

Ki-67 (%)	(#1) Benign hidradenoma	(#2) Atypical hidradenoma	(#3) Malignant hidradenoma	(#4) Metastasizing adnexal carcinoma
N	7	15	11	8
Median (range)	1.93 (0-6.8)	4.65 (2.36-11.45)	33.06 (13.95-47)	26.0 (7.15-40.8)
Mean	3.06	6.23	30.39	24.42

Conclusions: Our findings show that atypical hidradenoma has a significantly lower Ki-67 expression compared to the malignant counterpart and the metastasizing adnexal carcinoma, and only approaches statistical significance (p=0.045) compared to the benign hidradenoma group. The results suggest that these tumors are likely to recur but unlikely to metastasize. Ki-67 may be a helpful diagnostic adjunct in classifying hidradenoma in the setting of small biopsy specimen.

477 Malignant Neoplasms Affecting the Umbilicus: Clinicopathologic Features of 77 Tumors

JA Papalas, JF Madden, MA Selim. Duke University Medical Center, Durham, NC.

Background: The skin and subcutaneous tissues of the umbilicus are anatomically unique due to their proximity to intraabdominal and pelvic structures. In addition to primary skin malignancies, it is a site often involved with metastatic disease.

Design: We reviewed the clinical and pathologic features of 77 umbilical malignancies occurring at our institution since 1988.

Results: The population consists of 77 patients with a female:male ratio of 4.1:1.0 Average age is 63 years old for females and 55 years old for males. 88% (n=68) of malignancies originated outside the umbilicus while only 9 cases were primary skin tumors. Of patients with metastatic lesions, 84% of were female, and 16% were male. 58 (85%) patients with metastatic tumors had umbilical involvement from a known primary versus 10 (15%) patients who had unknown primaries. 9 patients (13%, 6 female/3male) with metastatic tumors to the umbilicus would present with solitary umbilical involvement. Of these 9 patients, 56% (n=5, all female) had clinically unidentifiable primary lesions. In females, the three most common primary sites were the ovary (n=22, average age 65 y/o), endometrium (n=6 average age 72 y/o), and pancreatobillary tree (n=4, average age 59 y/o). In males, the three most common primary sites were the genitourinary tract (n=4 average age 56 y/o), pancreatobillary tree (n=2, average age 72 y/o), and the gastrointestinal tract (n=2, average age 68 y/o). Of the primary umbilical malignancies, 44% of patients were male (n=4, average age

39 y/o) and 56% female (n=5, average age 49 y/o). Melanoma was the most common primary umbilical malignancy (n=6). Of these patients, 4 were female and 2 male. 2 lesions were in-situ, 1 lesion was Clark I, and 3 lesions were Clark IV. Average Breslow thickness was 2.05mm. The remainder of the primary umbilical tumors consisted of basal cell (n=1) and squamous cell (n=2) carcinomas.

Conclusions: Women with umbilical malignancies are older and much more frequently stricken than men. Metastases to the umbilicus are much more common than primary malignancy. The most likely primary site of a metastatic tumor to the umbilicus is the genitourinary tract. Most patients with metastases to the umbilicus have prior documentation of the primary malignancy. Rarely, patients present with metastatic tumors to the umbilicus. These patients are likely to have clinically unidentifiable primaries at the time of presentation. Patients with primary umbilical skin cancers are more evenly distributed across sex and are most likely have advanced malignant melanoma.

478 Clinicopathological & Immunohistochemical Features of Cutaneous Squamous Cell Carcinomas of the Lip

JZ Pat, RS Krause, M Raju, WH Leyva, AR Prasad. University of Arizona, Tucson, AZ; Southern Arizona VA Health Care System, Tucson, AZ; University of Washington, Seatle, WA.

Background: Cutaneous squamous cell carcinoma of the lip (CSCCL) typically has an aggressive behavior compared to CSCC involving other sites. There is a paucity of data regarding the clinical and immunohistomorphologic features of these aggressive tumors especially regarding microstaging parameters.

Design: Consecutive patients with CSCCL were identified from the clinicopathologic archives. Incidence of recurrence, metastasis, Co-morbid factors and mortality were noted. Histopathologic features and immunoprofiles were studied on formalin fixed, paraffin-embedded tissue.

Results: 46 patients had excisional biopsies for CSCCL (Lower lip=37, Upper lip=9). All were Caucasian males, age range 50 to 97 years (av. 75 yrs). 45/46 patients had altered immunity: Chronic leukemia (n=8), visceral malignancy (n=8), organ transplantation (n=4), chronic renal disease (n=7), diabetes (n=9), HIV (n=1), immunosuppressive treatment (n=9). Tumor size: 0.9 to 5.2 cm (av. 3.2cm). Tumor depth: <2mm (n=11), 2-6mm (n=26), >6mm (n=9). Differentiation: 9 poor, 26 moderate, 11 well differentiated. Tumor subtypes: acantholytic (n=3), desmoplastic (n=4), spindle cell (n=2). 27 tumors invaded the deep dermis, 12 were in the underlying muscle. 4 cases had regional lymph node metastases and 6 showed local recurrences, 3 of whom died of the disease. Vascular (n=10) and perineural (n=13) invasion were seen. Average mitotic activity was >4/10 hpf. 31 tumors had infiltrative pattern of growth. Tumor showed over expression of cyclin-D1 (43/46) and p53 (44/46), and decreased E-cadherin expression (36/46). The average Ki-67 proliferative index was 89% and correlated with increased depth of invasion (p<0.001). Recurrent tumors had a higher proportion of decreased E-cadherin expression (p=0.04).

Conclusions: 1. CSCCLtend to invade into the deep dermis and beyond with the majority deeper than 2mm. 2. Most tumors have an infiltrative growth pattern, majority are moderately to poorly differentiated. 3. CSCCL show over expression of cyclin-D1 and p53, with high Ki-67 proliferative index. E-cadherin expression is decreased. 4. All of the recurrent and fatal tumors were deeper than 6mm and were not well differentiated, hence microstaging of CSCCL employing histologic grade, level of invasion, and tumor thickness, with assessment of proliferative activity may offer a more accurate assessment of tumor prognosis.

479 Comparative Expression of CXCR3 Chemokine Receptor and Their Ligands (CXCL9, CXCL10 and CXCL11) in Cutaneous Melanoma Progression

A Pellin-Carcelen, D Ramos, J Martin, E Jorda, A Pellin, C Monteagudo. University of Valencia, Valencia, Spain; Hospital Clinico Universitario, Valencia, Spain.

Background: Human cutaneous melanoma is responsible for a high mortality due to their metastatic potential which is considerably increased when melanoma starts growing vertically. It has been widely hypothesized that chemokines and their receptors may influence tumor progression in a variety of cancer types. The expression of CXCR3, CXCL9, CXCL10 and CXCL11 in the melanoma microenvironment has been previously reported.

Design: Eighty-seven cryopreserved melanoma samples were distributed in 5 different groups based on the thickness of primary tumour and the type of metastasis [18 thin (≤1mm) primary tumors, 22 thick (>1mm) primary tumors, 18 in transit metastases, 16 lymph node metastases, and 13 distant metastases]. The expression of the target genes and the control gene 18S was evaluated by the RT-Realtime PCR technique. The statistical correlation between the gene expression in the five different groups of samples was analysed with the non parametric Mann-Whitney or Kruskal-Wallis tests.

Results: The expression of the four transcripts (CXCR3, CXCL9, CXCL10 and CXCL11) was significantly higher in primary tumors than in melanoma metastases as a whole and in distant metastasis in particular. The expression of CXCL10, CXCL11 and CXCR3, but not CXCL9, was higher in thin and in thick primary tumors than in "in transit" and lymph node metastases. According to the ligand versus receptor comparative expression, we found a higher proportion of CXCL9 in thin primary tumors and in distant metastasis than in thick primary melanomas.

Conclusions: Our results suggest that the interaction between CXCL10 and CXCL11 with CXCR3 should have a higher influence than that of CXCL9 in lymphatic tumor dissemination. In regard to the ligand versus receptor analysis, the higher expression values of CXCL9 in thin tumors and distant metastasis than in thick primary tumours may be responsible for retaining tumor cells in the former, or guiding tumor cells to specific metastatic sites in the later. *Performed with FIS PI07/1203 grant, from Fondo de Investigacion Sanitaria, Spain.*

480 Defining Histopathologic Criteria of Cutaneous Metastatic Melanomas: A Clinicopathologic Study of 160 Cases with Emphasis on the Morphologic Spectrum
JA Plaza, C Torres-Cabala, H Evans, H Diwan, VG Prieto. Medical College of Wisconsin, Milwaukee, WI; MD Anderson Cancer Center, Houston, TX.
Background: Metastatic melanoma is a common source of cutaneous metastasis. In up to 5% of patients, cutaneous metastasis can be the first manifestation of melanoma. The diagnosis of metastatic melanoma usually poses little diagnostic difficulty, but occasionally it can adopt unusual or unfamiliar appearances mimicking benign and malignant neoplasms (spindle cell carcinomas, atypical fibroxanthomas, blue nevi, dermatofibromas, leimoysarcomas, etc). In this study, we present 160 cases of cutaneous metastatic melanomas and thoroughly analyze their histomorphologic spectrum. To the best of our knowledge this is the largest series of cutaneous metastatic melanomas.
Design: 160 cases with metastatic melanoma to the skin were the basis of our study. Glass slides stained with H&E for each case were reviewed. Paraffin blocks or unstained slides were available for immunohistochemical studies in all cases. Metastases to areas with important drainage of lymph node such as axillary region or groin, or histological evidence of lymph node remnants were criteria for exclusion from the study. Direct extension from lymph nodes was also excluded.
Results: Cases were classified by anatomic site of metastasis, primary origin, age and sex. The patients were 97 men and 63 women ranging from 51 to 88 years (mean 69.5). The tumors were located in back, upper extremities, lower extremities, abdomen, and head and neck area. The tumors ranged in size from 0.8 cm to 3.0 cm. The majority of metastatic melanomas showed classic histomorphologic appearance. In up 21.6% of cases, the lesions mimicked blue nevus, dermatofibroma, metastatic carcinoma, malignant and benign vascular neoplasms, and smooth muscle neoplasms. In such cases, immunohistochemical studies were used to aid the diagnosis. All metastatic melanomas had high proliferative rate (with MIB-1) and patchy expression of HMB45 antigen.
Conclusions: The histologic diagnosis of cutaneous metastatic melanoma can pose difficulties for diagnosis, especially if there is an unknown primary neoplasm, requiring ancillary studies and reliable histomorphologic criteria to establish an accurate diagnosis.

481 Immunohistochemical Detection of Merkel Cell Polyoma Virus in Merkel Cell Carcinoma
MP Pulitzer, AA Jungbluth, Y Chang, P Moore, KJ Busam. Memorial Sloan-Kettering Cancer Center, New York, NY; Ludwig Cancer Research Institute, New York; University of Pittsburgh, Pittsburgh.
Background: A novel polyoma virus has recently been detected in Merkel cell carcinoma and found to be present in approximately 80% of tumor samples by molecular studies. A monoclonal antibody has been generated for the detection of Merkel cell polyoma virus by immunohistochemistry.
Design: Immunoperoxidase staining was performed with the novel monoclonal antibody 2B4 (produced against a predicted antigenic epitope on the Merkel cell polyomavirus encoded T antigen) using a tissue microarray of 36 Merkel cell carcinomas as well as 10 whole tumor sections, with five samples of conventional Merkel cell carcinomas and five lesions of combined cutaneous squamous cell and neuroendocrine carcinoma. Immunostaining was also performed for CK20.
Results: Using the tissue microarray samples, 27 of 36 Merkel cell carcinomas (75%) were immunoreactive for 2B4. 26 of the 27 immunopositive tumors showed positive nuclear staining in more than 75% of the tumor cells. None of the five combined neuroendocrine and squamous cell carcinomas, which were studied on sections with the entire tumor profile, and found to be CK20-positive in their invasive neuroendocrine component, showed positive immunostaining for 2B4.
Conclusions: The monoclonal antibody 2B4 permits the immunohistochemical detection of Merkel cell polyomavirus in archival material at a similar frequency as previously reported by PCR studies. Virus antigen can be detected in the majority, but not in all Merkel cell carcinomas. This observation suggests that there is some heterogeneity among tumors classified as Merkel cell carcinomas. The lack of immunoreactivity in any of the tested CK20-positive neuroendocrine carcinomas, which arose in association with a squamous cell carcinoma, suggests that the etiology and/or molecular pathway of the combined tumors is different from the majority of de novo Merkel cell carcinomas.

482 Differential Gene Expression in Normal Skin, Actinic Keratosis, and Squamous Cell Carcinoma
SH Ra, DS Cassarino, XM Li, SW Binder. UCLA Medical Center, Los Angeles, CA.
Background: Squamous cell carcinoma (SCC) is one of the most commonly diagnosed skin malignancies. However, several lesions clinically and histologically simulate cutaneous SCC, including actinic keratosis (AK), which poses a challenge to the clinical diagnosis. The goal of our study was to develop a gene expression-based diagnostic method to distinguish among SCC, AK, and normal skin.
Design: Five actinic keratoses, five squamous cell carcinomas, and five normal skins were used for gene expression profiling. RNA was extracted from the paraffin blocks and converted to the labeled cRNA targets for human U133plus2.0 array hybridizations. The data analyses were performed using DNA-Chip Analyzer (D-Chip). Thresholds for selecting significant genes were set at a relative difference >= 2-fold, absolute difference > 100 signal intensity units and p<0.05. Genes that simultaneously met all three criteria were considered as significant changes.
Results: Over 200 genes were differentially expressed between SCC and normal skin and between AK and normal skin. The majority of the differentially expressed genes were down-regulated. Although overall gene expression profile of AK is similar to that of SCC, a small group of signature genes were identified which can be potentially useful for clinical discrimination (see Table I, FC= Fold change).

Table I. Differential gene expression between normal skin, AK, and SCC

Sample	Total # of genes upregulated (>2FC)	Selected upregulated genes (FC)	Total # of genes downregulated (>2FC)	Selected downregulated genes (FC)
Normal skin vs. SCC	57	S100A7A, SERPINB13 (>5FC)	271	SCARA5, HBB, SCGB2A2, DCD (>60FC)
Normal skin vs. AK	21	S100A8, CCL18, CENTG3 (>4FC)	185	CNN1, SCGB2A2, DCD (>200FC)
AK vs. SCC	4	HOXC6, HOXC4 (>2.5FC)	8	NFIB, RPF6, RTN4 (>2FC)

Conclusions: The distinctive gene expression profile of the selected squamous lesions offers the ability to distinguish SCC from its simulants. This offers the possibility of utilizing the gene expression microarray as a future molecular diagnostic tool to distinguish between normal skin, preneoplastic conditions such as AK, and SCC. In addition, the differentially expressed genes could be potentially used as prognostic markers or targets for future treatment.

483 Clinical Testing for Microsatellite Instability and Loss of DNA Mismatch Repair in Sebaceous Neoplasms
KM Rumilla, KA Mensink, LA Erickson, TJ Flotte, SN Thibodeau, KC Halling. Mayo Clinic, Rochester, MN.
Background: Sebaceous neoplasms are a characteristic of the Muir-Torre variant of Hereditary Non- Polyposis Colorectal Cancer (HNPCC). These lesions are characterized by the presence of defective DNA mismatch repair (dMMR). dMMR is defined by the presence of high level of microsatellite instability (MSI-H) or by loss of protein expression for one the four main DNA mismatch repair enzymes (MLH1, MSH2, MSH6 and PMS2) as detected by immunohistochemistry (IHC). Both testing methods are often used to screen high risk patients for HNPCC.
Design: We have analyzed 58 consecutive sebaceous lesions analyzed from August 2001 to June 2008. The data we collected included tumor classification, grade, location, MSI and/or IHC testing and germline testing. These cases included 2 sebaceous hyperplasias, 13 sebaceous adenomas, 2 sebaceomas, and 41 sebaceous carcinomas.
Results: MSI-H was present in 25 of 34 (73.5%) sebaceous carcinomas, 6 of 11 (54.5%) sebaceous adenomas, 1 of 2 (50%) sebaceous hyperplasias and none of the sebaceomas. Only one sebaceous adenoma was MSI-L, the remaining 17 lesions were MSS. By IHC testing, loss of protein expression was seen in 30 of 40 (75%) sebaceous carcinomas, 7 of 12 (58.3%) sebaceous adenomas and 1 of 2 (50%) sebaceous hyperplasias. The remaining lesions tested showed normal expression. Of the 47 cases for which both MSI and IHC had been performed, 2 (4.3%) were discordant - MSI testing was MSS or MSI-L and IHC showed loss of protein expression. Follow-up testing on 20 (of 40) cases with dMMR yielded 9 (45%) mutations (6 in *MSH2,* 2 in *MSH6* and 1 in *MLH1)*. The two cases with mutations in *MSH6* were the discordant cases.
Conclusions: Our results show that by performing both methods of microsatellite instability testing occasional discordant cases are identified. The majority of mutations identified involved DNA mismatch repair genes *MSH2* and *MSH6*. However, the finding of germline mutations in the discordant cases is significant.

484 Neuropilin-2 Expression in Normal Tissues, Various Tumors, and Primary and Metastatic Melanomas
EC Rushing, MJ Keefe, S Khanna, AA Jungbluth, KJ Busam, RM Alani. The Sidney Kimmel Comprehensive Cancer Center at Johns Hopkins, Baltimore, MD; Cleveland Clinic, Cleveland, OH; Johns Hopkins University School of Medicine, Baltimore, MD; Ludwig Institute for Cancer Research, New York, NY; Memorial Sloan-Kettering Cancer Center, New York, NY.
Background: Neuropilin-2 (NRP2) is a cell surface receptor involved in angiogenesis and axonal guidance. It has recently been shown to be a critical mediator of tumor-associated lymphangiogenesis and blocking of NRP2 function in vivo was demonstrated to inhibit tumor cell metastasis. Melanomas are notorious for their ability to metastasize at a relatively early stage of development and lymphangiogenesis is implicated as a metastasis conduit. Since NRP2 expression is not well documented, we investigated NRP2 expression in normal tissues, various tumors and melanomas.
Design: We evaluated NRP2 expression in 62 independent cases of melanoma in order to determine expression patterns across primary and metastatic melanomas as well as different histologic melanoma variants. We also evaluated a panel of normal human tissues and select non-melanocytic tumors since these have not been broadly evaluated for NRP2 expression. NRP2 expression was assessed using immunohistochemical staining with a polyclonal antibody against NRP2 and evaluated for extent and intensity of staining by two independent readers. Further analysis was performed on scanned slides using the FRIDA image analysis software.
Results: Significant staining was noted in all melanoma subtypes evaluated with 60/62 cases staining positively for NRP2. Among the cases of melanomas evaluated, all tumors demonstrated moderate to high levels of NRP2 expression with the exception of desmoplastic melanomas and some spindle cell nodular melanomas. All melanomas demonstrated significantly higher expression of NRP2 versus other tumor types evaluated (p<0.0001), with the exception of renal cell carcinomas which were highly positive for NRP2 expression as were normal kidneys.
Conclusions: We conclude that melanomas express high levels of NRP2 which is significantly elevated relative to all other malignancies evaluated in this study, with the exception of renal cell carcinomas. NRP2 was highly expressed in the majority of melanomas excluding desmoplastic variants and may be useful in the diagnosis of disseminated disease or as a prognostic indicator.

485   CLA, TRAF1, BCL2, NFKB2, CD56, EMA and Fascin Expression in CD30+ Lymphoproliferative Disorders of the Skin
EM Sagatys, D Rezania, M Naghashpour, LF Glass, ME Kadin, HD Cualing. Moffitt Cancer Center, Tampa, FL; Genoptix Medical Laboratory, Carlsbad, CA; Roger Williams Hospital, Providence, RI.
Background: Lymphomatoid papulosis (LyP), primary cutaneous (pcALCL) and systemic anaplastic large cell lymphoma (sALCL) are CD30+ lymphoproliferative disorders (LPD) with overlapping morphology, but widely different behavior. This study examines the role of BCL2, CD56, cutaneous lymphocyte antigen (CLA, skin homing), EMA, Fascin, NFKB2, and tumor necrosis factor receptor (TNFR) associated factor 1 (TRAF1, intracellular trafficking) in differentiating CD30+ LPD in the skin.
Design: With IRB approval, formalin-fixed, paraffin-embedded biopsy specimens from 13 LyP, 9 pcALCL and 8 sALCL were selected from the MCC Archives from 2000-07. All cases were stained with the above antibodies using manufacturer's protocols. Manual morphometry and virtual flow cytometry were performed to quantitate antibody expression. Statistical analysis was performed using non-parametric analysis of variance (Kruskal-Wallis method).
Results:

Table 1. Mean±SD

	LyP	pcALCL	sALCL
BCL2	37.0±14.8	18.7±12.7	69.5±21.1
CLA	52.4±25.1	28.6±12.7	6.5±7.6
TRAF1	25.1±22.4	32.8±22.3	0.9±1.4
NFKB2	100.0±0	98.9±3.3	76.8±32.5
CD56	0.2±0.4	0.1±0.3	0
EMA	2.7±5.6	13.3±28.3	18.8±26.9
Fascin	16.4±12.7	47.6±31.7	43.1±44.7

There was no significant difference of TRAF1 between LyP and pcALCL (p>0.05), but significant differences between LyP and sALCL (p<0.01), and pcALCL and sALCL (p <0.001). CLA expression showed significant differences between LyP and pcALCL (p<0.05) and LyP and sALCL (p<0.001), with insignificant differences between pcALCL and sALCL (p>0.05). BCL2 showed significant differences between pcALCL and sALCL (p<0.001) but not between LyP and pcALCL (p>0.05) and LyP and sALCL (p>0.05). NFKB2 showed significant differences between LyP and sALCL (p<0.01) and pcALCL and sALCL (p<0.05). CD56 (p=0.5283), Fascin (p=0.2590), and EMA (p=0.1624) were not contributory.
Conclusions: There was significant differential expression of TRAF1 and CLA in LyP. TRAF1 was negative in sALCL. CLA differentiates LyP from pcALCL and sALCL. BCL2 may differentiate pcALCL from sALCL. NFKB2 may be useful in distinguishing pcALCL from sALCL. This study indicates potential utility of TRAF-1, CLA, BCL2 and possibly NFKB2 in separating systemic from primary cutaneous CD30+ LPD. CD56, Fascin and EMA were non-contributory.

486   Differential Expression, Diagnostic Utility, and Potential Pitfalls of CD34 in Cutaneous Neural Tumors
M Sanders, JC Malone, A Martin, S Lear, S Bahrami. University of Louisville, Louisville, KY.
Background: CD34 is a transmembrane protein expressed on a variety of cell types. Expression in normal peripheral nerve and peripheral nerve sheath tumors has been described and has pointed to a distinct CD34 cell population that is postulated to represent either a precursor cell or a supportive cell for Schwann cells. Immunohistochemistry plays a cardinal role in the evaluation of cutaneous soft tissue tumors, and CD34 is a commonly employed marker in an immunohistochemical panel. Our objective was to analyze CD34 expression in a variety of cutaneous neural tumors with special interest in its diagnostic utility and/or potential pitfalls in the general evaluation of a cutaneous soft tissue tumor.
Design: A retrospective review of cases of cutaneous neural tumors diagnosed between 2001 and 2008 was performed at the University of Louisville in the department of dermatopathology. Slides were reviewed for confirmation of diagnosis and tissue quantity. Immunoperoxidase staining for CD34 was performed. Stromal and cellular staining for CD34 were stratified for the percentage of cells stained: For stroma, less than 1/3 of tumor immunopositive (1+), 1/3 – 2/3 of tumor (2+), and greater than 2/3 of tumor (3+); for cellular, less than 50% immunopositive (1+) and greater than 50% (2+).
Results: A total of 42 cases were stained for CD34 with the following diagnosis: palisaded encapsulated neuroma (PEN) (n=7), schwannoma (n=10), cellular schwannoma (n=1), neurofibroma (n=7), diffuse neurofibroma (n=3), malignant peripheral nerve sheath tumor (MPNST) (n=2), neurothekeoma (n=1), cellular neurothekeoma (n=3), granular cell tumor (GCT) (n=6), Morton's neuroma (n=1), and amputation neuroma (n=1). Average staining intensities for stroma were 1+ for MPNST, neurothekeoma including the cellular variant and GCT, 2+ for PEN, schwannoma and Morton's neuroma, and 3+ for neurofibroma including diffuse variants, cellular schwannoma and amputation neuroma. Cellular staining ranged from no staining in GCT to 2+ in cellular schwannoma and 1+ in the remaining neural tumors.
Conclusions: Neurofibromas, including the diffuse variant, consistently exhibit strong and diffuse stromal staining for CD34. This information should be helpful in the work up of cutaneous soft tissue tumors, when placing diffuse neurofibroma high on the differential diagnosis, and diagnostic error may be avoided when considering other CD34+ cutaneous soft tissue tumors.

487   Expression of CDK-2 in Psoriasis
A Santos-Briz, P Antunez, M Roncero, E Fernandez, A Bullon, P Unamuno. Hospital Universitario de Salamanca, Salamanca, Spain.
Background: Psoriasis is a chronic inflammatory skin disease characterized histologically by hyperproliferation and aberrant differentiation of epidermal keratinocytes. It is known that Cyclin-dependent kinase 2 (CDK2) plays an important role in keratinocyte proliferation. The aim of our study was to evaluate the expression of CDK-2 in cutaneous specimens of patients with psoriasis and compare it with normal skin and other inflammatory dermatosis.
Design: The immunohistochemical expression of CDK-2 was evaluated in cutaneous biopsies from a group of 71 patients with psoriaris, 18 of them with palmoplantar psoriaris. Results were compared with the expression of CDK2 in normal skin (n=40), eczema (n=28), cutaneous lupus erythematosus (n=16), pityriasis rosea (n=10), and chronic lichenoid pityriasis (n=11). For our purpose a high throughput Tissue Microarray strategy was designed.
Results: Increased expression of CDK2 was found in the upper layers of the lesional psoriatic epidermis compared to epidermis in both normal skin and other inflammatory dermatosis (p<0,001). Expression also differed among conventional psoriasis and palmoplantar psoriasis (p<0,001). CDK2 expression was found in 66% of psoriasis, 11.8% of palmoplantar psoriaris, 25.9% of eczemas, 0% of cutaneous lupus erythematosus, 10% of pityriasis rosea , 9.1% of chronic lichenoid pityriasis and 9% of normal skin samples.
Conclusions: Our results suggest that CDK2 plays an important role in keratinocyte proliferation in psoriasis. Moreover, differences between the expression of conventional psoriasis and palmoplantar psoriasis specimens suggest a different pathogenesis of both diseases.

488   Merkel Cell Carcinoma of the Skin: A New Type of Virus-Associated Human Tumour
X Sastre-Garau, M Peter, MF Avril, H Laude, J Couturier, F Rozenberg, A Almeida, F Boitier, A Carlotti, B Couturaud, N Dupin. Institut Curie, Paris, France; Groupe Hospitalier Cochin-St Vincent de Paul, Paris, France.
Background: Merkel cell carcinoma (MCC), a skin tumour with neuro-endocrine features, was recently found to be associated with a new type of human polyomavirus, called Merkel Cell Virus (MCV). We investigated the specificity of this association as well as a causal role of MCV in oncogenesis.
Design: In this work, DNA and RNA from 10 cases of MCC were analysed using PCR and RT-PCR. DNA from 1241 specimens of a wide range of human tumours was also analysed. The DIPS technique was used to identify the integration locus of viral DNA sequences. Array-CGH was performed to analyse structural alterations of the cell genome.
Results: MCV DNA sequences were found in all 10 cases of MCC and in none of the 1241 specimens of other tumour types. Clonal integration of MCV into the host genome was seen in all MCC cases. A recurrent pattern of conserved viral sequences which encompassed the replication origin, the small tumour (ST) and the 5' part of the large tumour (LT) antigen DNA sequences was observed. Both ST and LT viral sequences were found to be significantly expressed in all MCC. Neither recurrent site of integration nor alteration of cellular genes located near the viral sequences were observed.
Conclusions: The tight association of MCV with MCC, the clonal pattern of MCV integration as well as the expression of the viral oncoproteins strongly support a causative role for MCV in the tumour process. This information will help the development of novel approaches for assessment and therapy of MCC and biologically related tumours.

489   E-Cadherin and β-Catenin Are Dysregulated in Merkel Cell Carcinomas
S Serra, D Ghazarian, R Chetty. UHN, University of Toronto, Toronto, Canada.
Background: Adhesion molecules are involved in epithelial integrity and polarity function. β-catenin acts as adhesion molecule and transcription factor in the Wnt pathway. It interacts with E-cadherin, a transmembrane adhesion molecule also involved in cell-to-cell contact.
Design: The aim of the study was to examine the expression of β-catenin and E-cadherin in Merkel cell carcinomas (MCC). Twenty-six MCC were retrieved from the archives of the Department of Pathology, UHN, and stained with β-catenin and two antibodies (Ab) (against extracellular and cytoplasmic domains) to E-cadherin. Location of reactivity (membranous, cytoplasmic, nuclear), percentage of positive cells (<5%, ≥5-30%, >30%-70% and >70%, scored from 0 to 3, respectively) and intensity (negative, weak, moderate and strong; from 0 to 3, respectively) were recorded for both molecules.
Results: Of the 26 biopsies, 15 were males, aged from 59 to 96 years (average 69). Twenty MCC were primary tumors of the skin, 2 of the lip, 3 metastases to lymph nodes and 1 to the tonsil. The E-cadherin Ab recognizing the extracellular domain showed cytoplasmic positivity in 57.6% (15/26) of the cases, cytoplasmic/membranous in 1 and negative in 10 (38.4%). The intensity was weak in 12/26 (46%) cases and strong in 1. Eight of 26 (30.7%) cases showed 5-30% of the cells to be immunoreactive and 7/26 (27%) >30-70%. The immunoreactivity of the Ab against the cytoplasmic domain of E-cadherin was nuclear in 11/25 (44%) cases, nuclear/cytoplasmic in 8/25 (32%) and cytoplasmic only in 5/25 (20%), 1/25 case was negative and no tissue was available in one case. The intensity of the staining was strong in 12/25 (48%) and weak in 3/25 (12%) cases. In 19/25 (76%) cases, more than 70% of the tumors cells were positive with this Ab. Sixteen of 26 (61.5%) cases showed cytoplasmic immunoreactivity for β-catenin, 27% (7/26) both cytoplasmic and nuclear and 11.5% (3/26) both cytoplasmic and membranous.The intensity of the immunoreaction was strong in 7/26 (27%) and weak in 3/26 (11.5%) cases. The majority of tumors showed immunoreactivity in 30-70% of cells.
Conclusions: Both β-catenin and E-cadherin are dysregulated in all cases of MCC, with a loss of the normal membranous pattern and redistribution to the cytoplasm and nucleus. In addition, the staining pattern for E-cadherin depends on the type of E-cadherin Ab used. The Ab that recognizes the extracellular domain of the E-cadherin molecule results in loss of staining in some cases or cytoplasmic immunoreactivity, while the Ab against the cytoplasmic domain results in cytoplasmic and/or nuclear positivity.

490 Insulin-Like Growth Factor-II Messenger RNA Binding Protein-3 (IMP-3) Expression in Nodal Nevi and Metastatic Melanoma
R Sharma, M Pletneva, PB Illei. Johns Hopkins Medical Institutions, Baltimore, MD.
Background: IMP-3 is expressed during embryogenesis and several malignant epithelial tumors. Recently, IMP-3 expression was reported in primary and metastatic melanomas but not in cutaneous nevi including atypical nevi (Mod Pathol, 2008; 21: 431-437) with higher expression levels in metastatic tumors. The presence of nodal nevi primarily in axillary and inguinal lymph nodes can pose a diagnostic difficulty especially in sentinel lymph nodes. In some cases, immunohistochemistry for Melan-A and Hmb-45 cannot distinguish between beni nevi and micrometastic melanoma.
Design: We have performed immunohistochemistry for Melan-A, Hmb45 and IMP-3 (DAKO, Carpintera, CA) in 9 lymph nodes with nodal nevi and 12 lymph nodes involved by metastaic melanoma.
Results: All 9 nevi and all 12 melanomas were Melan-A positive. All 12 melanomas were Hmb45 positive and weak staining was also seen three nodal nevi. IMP-3 postivity was seen in 11 of 12 melanomas and focal weak staining in 1 of 9 nodal nevi.
Conclusions: Based on the limited number of cases in this pilot study immunohistochemistry for IMP-3 could be helpful in differentiating benign nodal cells from micrometastatic melanoma.

491 The Value of Nuclear Morphometry in Malignant Versus Benign Parakeratosis
J Song, CR Shea. University of Chicago, Chicago.
Background: Shave biopsies of skin, despite being convenient and minimally invasive, can sometimes have inadequate depth. A shave biopsy composed mainly of stratum corneum can pose a diagnostic challenge. Parakeratosis occurs in both benign and malignant diseases. Even though parakeratotic nuclei are often pyknotic, malignant ones do appear somewhat atypical in our experience. Nuclear morphometry could provide relevant information in these cases, an approach that has not been investigated in the literature. In this context, we studied the value of nuclear morphometry of parakeratosis in routine H&E slides from benign and malignant skin biopsies.
Design: Squamous cell carcinoma (SCC) and psoriasiform dermatitis (PD) cases with significant parakeratosis were selected during a 2-month period (12 SCC, 14 PD). Digital images (400 X, 1300 x 1030 pixels) were taken in parakeratotic areas of stratum corneum. Nuclear identification and morphometry were performed using the automated, open-source software CellProfiler running on an Intel PC. Statistical analysis was conducted by t-test.
Results: Each case had 126 to 768 well-visualized parakeratotic nuclei (mean 337). Significant differences were found between SCC and PD in nuclear area, area variability (the standard deviation among all nuclei of one case), form factor, and short axis (Table 1). Form factor, defined as (4 pi) Area/Perimeter^2, correlates with nuclear convolution or indentation (1 for perfectly round objects). Nuclear area alone could discriminate between most cases of SCC and PD. There was not much difference between SCC and PD in nuclear perimeter or long axis, probably because all parakeratotic nuclei, including benign ones, tend to be elongated.

Table 1. Nuclear morphometric parameters.

Parameter (Mean ± SD)	SCC	PD	P value
Area	355 ± 75	234 ± 45	< 0.0001
Area Variability	176 ± 51	92 ± 28	< 0.0001
Perimeter	86 ± 11	78 ± 6	0.02
Form factor	0.57 ± 0.1	0.47 ± 0.07	0.005
Long Axis	36 ± 6	35 ± 3	0.57
Short Axis	12 ± 2	8 ± 1	< 0.0001

Unit, pixel (1 pixel = 0.22 micron).
Conclusions: Nuclear morphometry may provide valuable objective information in the differential diagnosis of benign and malignant parakeratosis, a situation that may be encountered in very superficial shave biopsies. Accurate morphometry can be performed with free, open-source software, and requires little special knowledge of image analsysi or programming, making it an affordable and widely adaptable approach.

492 C-kit Expression in Cutaneous Melanoma. In Vitro Effects of Drugs Targeting C-kit
A Sorolla, M Mayorga, A Yeramian, AM Perez de Santos, A Velasco, R Egido, L Abal, X Matias-Guiu, RM Marti. Hospital Universitari Arnau de Vilanova, Lleida, Spain.
Background: Melanocytes express c-kit. However, the significance c-kit expression in melanoma, and the in vitro effects of drugs targeting c-kit in melanoma are under debate.
Design: c-kit expression was assessed by immunohistochemistry (IHC) in formalin-fixed, paraffin-embedded biopsies of cutaneous melanoma (primary and metastasis), and in 19 original cell lines. C-kit mutation analysis was done in the cell lines. Cell lines were treated with tyrosine kinase inhibitors (imatinib mesylate, sunitinib), and proteasome inhibitors (bortezomib, and MG123). Cell viability, cell proliferation and apoptosis, were evaluated.
Results: c-kit was frequently expressed in melanoma (68 % primary tumors, 62 % metastasis, 68 % cell lines). In primary tumors, the expression was higher in tumor cells located in the surface of the lesions. In some cases, the expression pattern was similar in the primary tumor and the corresponding metastasis. C-kit mutations were not found. Imatinib mesylate treatment showed a clear reduction of viability in 8 of 19 cell lines (42%). Sunitinib decreased cell viability (up to 60%) in some cell lines. Proteasome inhibitors reduced cell survival in a dose-dependent manner in the majority of cell lines tested. A combined treatment of bortezomib and sunitinib showed either additive or synergistic effects on inhibition of cell growth.
Conclusions: The results confirm the frequent expression of c-kit. Results of in vitro treatment with drugs targeting c-kit supports the hypothesis that these drugs could be of some help in the treatment of patients with disseminated cutaneous melanoma.

493 CD34 Staining in Neurofibromas: A Diagnostic Pitfall
JM Uchin, BP Rubin, JR Goldblum, SD Billings. Cleveland Clinic, Cleveland, OH.
Background: Neurofibromas are benign neoplasms that have three well-documented growth patterns: localized, diffuse, and plexiform. We have reviewed many outside consultation cases in which neurofibromas were misdiagnosed as dermatofibrosarcoma protuberans (DFSP). Almost uniformly, the misdiagnosis was caused by misinterpretation of positive CD34 staining. Herein we describe the CD34 staining patterns of 44 excised neurofibromas.
Design: 16 cases of localized neurofibromas, 10 cases of plexiform neurofibromas, and 18 cases of diffuse neurofibromas were retrieved from archives. H&E slides were reviewed by 3 soft tissue pathologists and their diagnoses confirmed. Immunohistochemistry for CD34 (QBEnd/10, Ventana Medical Systems) using DAB. Cases were scored according to a semi-quantitative scale: 0 (negative staining), 1+ (< 25% staining), 2+ (25-50% staining), 3+ (> 50% staining).
Results: The IHC staining results are summarized in the table below. Localized neurofibromas ubiquitously demonstrate staining with CD34, in a predominantly widespread pattern. While diffuse and plexiform neurofibromas showed more variation in their CD34 staining patterns, ranging from widespread to focal to patchy, 96% of these subtypes expressed CD34.

CD34 Staining Results

Score	Localized NF	Plexiform NF	Diffuse NF
0	0	0	1
1+	0	3	4
2+	1	0	3
3+	15	7	10
Overall (+)	16/16 (100%)	10/10 (100%)	17/18 (94%)

Conclusions: Significant histological and immunohistochemical overlap can exist between neurofibroma and DFSP. In DFSP, immunoreactivity for CD34 can be crucial in establishing the diagnosis in small biopsies or challenging morphologic variants (e.g. myxoid DFSP). Our data demonstrate significant, often diffuse CD34 expression in all subtypes of neurofibroma. Awareness of this potential diagnostic pitfall can prevent misdiagnosis. This is especially true in the setting of diffuse neurofibroma- which shows significant histiologic overlap with myxoid DFSP, and with small biopsies of solitary neurofibroma. In addition, our data show that CD34 can be used as an additional reliable diagnostic marker for all morphologic variants of neurofibroma.

494 Evaluation of the Impact of International Society for Cutaneous Lymphoma (ISCL) Scoring Algorithm on Diagnosis of Early Mycosis Fungoides
H Vakil, M Raoufi, P Sochacki, N Khoury, W Pfeifer, E Levi. Wayne State University, Detroit, MI; Henry Ford Hospital, Detroit, MI; VA Medical Center, Detroit, MI; Boston University, Boston, MA.
Background: Recently, ISCL proposed a scoring algorithm for diagnosis of early Mycosis Fungoides (MF), incorporating clinical, histopathologic, molecular and immunopathologic criteria. However, specifying the histopathologic features by which the early MF may be differentied from inflammatory diseases is still challenging, controversial and yet crucial issue. This study is designed to evaluate how the algorithm proposed by ISCL for scoring histopathologic criteria may affect the interpertation of early lesions of MF.
Design: We selected 20 patients from our archives (1992-2008) with known MF, and total number of 30 biopsies (including the ones which were not originally diagnosed as MF) were retrieved. We also added 10 cases of benign dermatoses from patients with no history of MF. Two pathologists were asked to blindly score all 40 biopsies based on the ISCL histopathologic criteria (epidermotropism without spongiosis, and lymphoid atypia). After the blinded scoring, the clinical and laboratory data were incorporated, and the initial diagnoses were reassessed based on ISCL scoring criteria. We investigated the inter-rater agreement for each of these two criteria, as well as for the final diagnoses.
Results: The inter-rater agreement (kappa coefficinet) for "epidermotropism without spongiosis" was 0.31, for "lymphoid atypia" 0.41, and for diagnosis of MF 0.45. After comparing the diagnoses made by two pathologists with original ones, 13% and 43% of cases were upstaged from early benign dignosis to MF. Interstingly, only one out of ten cases of benign dermatoses was diagnosed as MF by one of the pathologists. The most common diagnoses in prior biopsies were subacute eczematous dermatitis (10%), poikiloderma (10%), and fixed drug erruption (6.7%).
Conclusions: This study shows that application of algorithm proposed by ISCL for scoring histopathologic criteria contribute to improve the diagnostic yield for early lesions of MF, and upstage the diagnoses in a significant number of cases which were primarily diagnosed as benign lesions. However, it is worth to note that utility of histopathologic criteria is preserved by the interdependence on the other diagnostic criteria proposed by ISCL, i.e. clinical, molecular, and immunopathologic to establish the diagnosis of early MF.

495 Immunopathological Features of Cutaneous Squamous Cell Carcinomas in Immunocompromised Patients
CM Valentino, R Krouse, D Bradely-Dunlop, R Nagle, E Akporiaye, A Prasad. University of Arizona, Tucson, AZ; United States Department of Veteran Affairs, Tucson, AZ.
Background: An immunocompromised (IC) state may contribute to the increased development of cutaneous squamous cell carcinoma (CSCC). This study is an initial evaluation of the immunologic & histopathological differences within CSCC arising in IC and non-IC patients.
Design: Twenty cases of CSCC were included in this study (10 IC and 10 non-IC). An IC state was due to immunosuppressive therapy or underlying disease. Histological features i.e. size and depth of tumor, and degree of differentiation were studied. Immunohistochemical analysis was performed using antibodies against CD4, CD8,

CD1a, HLA-G, CD83, CD207, and Granzyme B. Paired student t-test statistical analysis was used to evaluate data.
Results: There was no difference in age and site between IC and non-IC patients. CSCC in IC patients had an average size of 1.9cm. vs 1.5cm. in non-IC patients. Tumors in the IC group invaded deeper (6 mm. vs 3mm.). 7/10 CSCC in the IC group were moderately to poorly differentiated, 3 were well differentiated. 6 of 10 tumors in the non-IC group were well differentiated, and the remaining four were moderately differentiated. There was a trend towards increased numbers of CD4 (p=0.056) and CD8 (p=0.0489) T cells in tumor tissue compared to normal tissue in both groups. There was an increased ratio of CD4:CD8 T cells (p=0.021) in the adjacent normal skin in non IC patients however there was an almost 5 fold decrease in CD4: CD8 ratio within the tumor of non IC group compared to the IC group reflecting an increased number of CD8 positive T cells in the tumor of both groups. Though there was a modest increase in CD1a positive dendritic cells in tumor and adjacent normal tissue of non-IC patients, there was a decreased number of CD207 positive Langerhans cells in the tumors of both groups. CD83 staining was minimal and correlated with the absence of Granzyme B staining in the tumor and normal skin of both groups.
Conclusions: CSCC in Immunocompromised individuals tend to be larger and invade to a greater depth. These tumors are more non well differentiated compared to CSCC in non-IC patients. These data suggest a lack of effector anti-tumor function at the tumor site in both groups that may contribute to tumor progression. Unlike previous reports, no staining was observed in SCC tumor tissue from both groups for non-classical HLA-G, which has been associated with tolerance induction reflecting a negative immune regulatory role in CSCC.

496 Pathologic Spectrum of Papulosquamous and Pustular Skin Reactions during Anti-TNF Therapy
EF Velazquez, RA Vleugels, AA Qureshi. Brigham and Women's Hospital, Harvard Medical School, Boston, MA.
Background: Anti- tumor necrosis factor inhibitors (anti-TNF biologic drugs), currently used to treat different autoimmune conditions, may be associated with cutaneous drug reactions. Clinically, new onset eruptions, worsening of known psoriasis and psoriasiform drug reactions have been reported. However, not much is known about the different histopathologic patterns of such skin reactions. The aim of this study was to evaluate the pathologic spectrum of clinically papulosquamous to pustular lesions in this setting.
Design: A total of 14 skin biopsies from 8 patients (7 females and 1 male with a mean age of 51 years) under anti-TNF-therapy for autoimmune disease (7 with rheumatoid arthritis and 1 with Crohn's disease) who developed a scaly erythematous to pustular skin rash during treatment were included in this study. None of these patients had history of psoriasis or lichen planus.
Results: Nine biopsies (5 patients) showed a pattern similar to psoriasis that varied from that seen in early or "guttate" lesions (3 biopsies), to well-established psoriasis (4 biopsies) to pustular psoriasis (2 biopsies). Eosinophils in the infiltrate varied from none (1 biopsy) to few/up to 1 per 5 HPF (6 biopsies) to easily identified/more than 1 per 5 HPF (2 biopsies). Three biopsies (2 patients) showed a lichenoid dermatitis with epidermal hyperplasia, hypergranulosis and a band-like lymphoid infiltrate with numerous Civatte bodies similar to lichen planus. Both lichenoid cases showed numerous plasma cells with none to few eosinophils in the infiltrate; Steiner stains were negative. Two biopsies (2 patients) showed sterile pustular folliculitis with a mostly neutrophilic infiltrate. PAS-D was negative for fungi in all cases.
Conclusions: Anti-TNF biologic drugs elicit a spectrum of drug reactions that go beyond the eosinophilic-rich hypersensitivity reaction classically associated with drugs and may closely mimic primary dermatitis. We describe here several cases that histopathologically mimic a spectrum of psoriasis (from early "guttate" to pustular) and lichen planus. Two cases of sterile pustular folliculitis were also observed. To our knowledge lichen-planus like dermatitis and sterile pustular folliculitis were not previously described in this setting and should be included in the list of anti-TNF-related drug reactions. Because the differential histopathological findings may be subtle and eosinophils rare, clinical correlation is crucial to make the diagnosis of anti-TNF related drug reactions.

497 Cutaneous Squamous Cell Carcinoma (CSCC) – One Year Experience of a Single Dermatopathology Service at a University Based Academic Medical Center
RK Virk, R Han, A Deng. UMass Memorial Hospital, Worcester, MA.
Background: Cutaneous squamous cell carcinoma (CSCC) is the second most common non-melanocytic skin cancer and the incidence is on the rise. Although the prognosis for CSCC is usually excellent, a small subset of tumors do recur, metastasize, and even cause death. It is thus crucial to accurately identify the subset of CSCC patients at risk for poor outcomes.
Design: We reviewed all the CSCC cases from a single dermatopathology service of an academic medical center during the period of July 2007 to June 2008.
Results: Our findings are: **1)** Of the total 15,000 specimens, 1421 were diagnosed as squamous cell tumors (approximately 9 %). Among all squamous cell lesions, 54% (n=763) were squamous cell carcinoma in-situ (SCCIS) and 46% (n=661) were invasive squamous cell carcinomas. **2)** Among the invasive CSCC, 53.4% (n=353) cases were present on the head and neck; 40% (n=263) were from the extremities, 9.5% (n=62) cases on the ear; and the trunk counted only for < 7% cases. **3)** The mean age of invasive CSCC was 76 years (range 40-100 years) which was similar to mean age for in-situ lesions (mean age- 74 yrs). Overall male to female ratio was 2:1. However, poorly differentiated CSCC showed 9:1 male to female ratio, significantly different from overall ratio. **4)** Most invasive carcinoma cases were well differentiated (WD) (71%, n=470), followed by moderately differentiated (MD) (20%, n=129), and then poorly differentiated (PD) (3%, n=20). Still, some were difficult to classify (6%, n=42). **5)** 69% CSCC on the head and neck were well differentiated, whereas moderately

differentiated and poorly differentiated accounted for 26% and 5% respectively. The distribution of WD, MD and PD CSCCs on the extremities was: 78%, 13% and PD 2% respectively. Head and neck region had more proportion of poorly differentiated CSCCs relative to extremities. **6)** The degree of differentiation was reversely associated with the possibility of having multiple skin cancers: PD 25% > MD 13% >WD 4% respectively. **7)** 11% of all CSCCs cases were associated with coexisting basal cell carcinoma (BCC). However, we did not find any correlation between the degree of differentiation of CSCCs and presence of BCC.
Conclusions: The head and neck regions had more proportion of poorly differentiated CSCC which are associated with multiple skin cancers.

498 Early-Onset Lichenoid Graft-Versus-Host Disease: A Unique Variant of Acute Graft-Versus-Host Disease Occuring in Peripheral Blood Stem Cell Transplant Recipients
HJ Votava, CM Magro. New York University School of Medicine, New York, NY; Weill Medical College of Cornell University, New York, NY.
Background: Hematopoietic stem cell transplants define an important therapeutic role in the treatment of hematologic malignancies, along with hematologic and immunologic deficiencies. One of the greatest rate limiting factors in its long-term success is chronic graft-versus-host disease (GvHD), a multi-organ process that closely recapitulates autoimmune disease. Although the term chronic GvHD suggests an insidious process developing at least several months after transplantation, there are increasing reports describing its earlier onset.
Design: The purpose of this study was to identify early onset lichenoid GVHD as a potential complication of allogeneic peripheral stem cell transplantation and to determine the origin of the lymphocytic infiltrate present in biopsy specimens of early-onset lichenoid GvHD. A retrospective study identified patients diagnosed with early-onset lichenoid GvHD. An attempt was made to correlate this diagnosis with the nature of the transplant received and concurrent or prior episodes of acute GvHD. The nature of the infiltrating lymphocytes was explored using a fluorescent in situ hybridization (FISH) XY assay.
Results: Patients in whom a sex mismatch was present between donor and recipient were included, representing a study population of 17. All patients had received an allogeneic peripheral blood stem cell transplant (PBSCT). All patients had biopsy proven lichenoid GvHD morphologically indistinguishable from lichenoid chronic graft versus host disease. All patients had prior episodes of acute GvHD, which was biopsy proven in 10 cases. FISH XY studies revealed that the infiltrating lymphocytes were of donor origin in 11 of the cases.
Conclusions: Early-onset lichenoid GvHD is a phenomenon characteristic of PBSCT setting and appears to be mediated by donor lymphocytes reflecting the higher numbers of donor T cells encountered in PBSCT, compared with bone marrow transplant recipients. We consider this reaction pattern a distinctive and unique subtype of acute graft versus host disease.

499 Stem Cell-Associated Markers Are Useful in Distinguishing Melanoma from Nevi
D Wagner, G Scott, Q Yang, J Huang. University of Rochester Medical Center, Rochester, NY; UCLA School of Medicine, Los Angeles, CA.
Background: Distinguishing melanoma from nevi can be difficult in certain cases. A previously published study showed that stem cell marker EZH2 is frequently expressed in melanoma but very rarely in nevi. Since EZH2 is a polycomb gene involved in controlling cell proliferation, this finding suggests possible molecular pathway in melanoma as well as providing a useful tool in the differential diagnosis of difficult cases. We studied additional stem cell-associated markers as well as EZH2 in a large cohort of melanoma and nevi.
Design: Two tissue microarrays (TMA) were constructed consisting of 80 cases of primary melanoma, 74 cases of metastatic melanoma and 76 cases of nevi. Sections were stained with antibodies for: Bmi-1 (Upstate, 1:100), EZH2 (VisionBio, 1:100), CD44 (eBioScience, 1:1000), SOX2 (R&DSystems, 1:100) and OCT3/4 (BioCare, prediluted). Only intact cores were scored.
Results: Among the stem cell associated markers studied, SOX2 and EZH2 were frequently overexpressed in primary and metastatic melanomas in comparison to nevi (p<0.001). The other three markers showed no difference among the groups. The results are summarized in Table 1.

Expression of stem cell-associated markers in melanoma, metastatic melanoma and nevi (positive/total (%positive))

	Oct3/4	Bmi1	SOX2	EZH2	CD44
Melanoma	0/78 (0%)	0/80 (0%)	55/69 (80%)	68/78 (87%)	77/77 (100%)
Metastatic Melanoma	0/73 (0%)	0/74 (0%)	42/73 (57%)	67/70 (96%)	70/70 (100%)
Nevi	0/77 (0%)	0/76 (0%)	13/72 (18%)	9/69 (13%)	72/72 (100%)

Conclusions: In addition to EZH2, we have identified another stem-cell associated marker SOX2 which is frequently overexpressed in primary and metastatic melanomas but infrequently in nevi. SOX2 is a transcription factor involved in the regulation of embryonic development and in the determination of cell fate which is essential to maintain self-renewal of undifferentiated embryonic stem cells. It will be important to determine if EZH2 and SOX2 function in the same pathway or different pathways to regulate melanoma cell growth. A combination of both markers provide high sensitivity and specificity in the differential dioagnosis of melanoma from nevi. Bmi1, CD44 and Oct3/4 are not differentialy expressed in the two lesions.

500 Graft-Versus-Host Disease Has Feature of T Cells, B Cells, and Systemic Sclerosis: A Study of Cytokine Expression in Histologically Matched Skin Biopsies
JM Wu, CJ Thoburn, J Wisell, AD Hess. Johns Hopkins Hospital, Baltimore, MD.
Background: Graft-versus-host disease (GVHD) is the leading cause of non-relapse mortality after allogeneic bone marrow transplantation (BMT). Although the clinical presentation is well-characterized, much remains to be elucidated in the context of pathogenesis.
Design: Forty-seven skin biopsies representing GVHD grades 0, I, II, III, lichenoid (L), and sclerodermoid (S) were included from 31 patients with previous allogeneic BMT. Paraffin embedded tissue was harvested for cDNA. Real-time polymerase chain reaction assessed levels of the following markers: 1) T and B cells: CD3, CD20; 2) T cell subsets: Foxp3, TGFß, IL-17; 3) cytokines associated with GVHD: interferon-gamma (IFNγ), IL-6; 4) factors implicated in systemic sclerosis: connective tissue growth factor (CTGF), allograft inflammatory factor-1 (AIF-1), and IL-13. Expression was correlated to grade, length of survival, and overall survival. Statistical analysis was performed using logistic and linear regressions.
Results: Levels of two markers significantly correlated with length of survival (TGFß, corr coeff -23.6, p=0.009 and AIF-1, 14.0, p=0.035), while IFNγ approached statistical significance (-11.2, p=0.076). Levels of the same three markers also correlated with histologic grade by inspection, but did not reach statistical significance: IFNγ (0, 0.251, I, 0.599, II, 0.767, III, 0.496, L, 1.02, S, 0.382, p=0.097), TGFß (0, 0.396, I, 0.544, II, 0.876, III, 0.570, L, 0.926, S, 173.6, p=0.13), and AIF-1 (0, 0.124, III, 0.006, L, 0.728, S, 0.718, p=0.527). No correlation to diagnosis or survival was found with CD3, Foxp3, IL-6, and CTGF. Expression of IL-17, IL-13, and CTGF was not detected. Lastly, expression of CD20 was observed in 2 of 9 patients with lichenoid GVHD.
Conclusions: We identify 3 markers that are not only potentially implicated in the progression from acute to chronic GVHD, but also modulate survival after transplantation, rendering IFNγ, AIF-1, and TGFß promising therapeutic targets. A second target is identified in a subset of patients with lichenoid GVHD. The presence of CD20 positive B cells may correlate with the recently described group of chronic GVHD patients who are responsive to rituximab. Our findings challenge the notion that GVHD is a uniform, T cell driven process. Rather, there appears to be subsets within GVHD patients, whose disease manifestation rests with the interplay of T and B cells, as well as factors involved in systemic sclerosis.

Education

501 What Are the Pathology Education Requirements for All Clinical ACGME Accredited Programs in an Academic Center?
SM Bean, A Nagler, PJ Buckley. Duke University Medical Center, Durham, NC.
Background: The Accreditation Council for Graduate Medical Education(ACGME) recognizes that knowledge of pathology is integral to the practice of medicine and mandates pathology education for many accredited programs. At academic centers, the pathology department commonly provides this required education for clinical trainees. This study determines the institution-wide pathology education GME requirements (exclusive of pathology residency and fellowships) in an academic center.
Design: Key word searches for "pathology," "laboratory," "autopsy," and "morbidity" were performed on all clinical Residency Review Committees (RRC) program requirements documents. A determination was made as to whether a pathology education requirement was identified for each search occurrence. Requirements were categorized.
Results: ACGME lists 102 clinical programs; 74 exist at Duke. Fifty-six (76%) programs had requirements.

Table 1. Pathology education requirements for clinical ACGME accredited programs at a single academic center.

Pathology Education Requirements	Number(%)
Consultation/Support	29(40%)
Teaching/Conferences	37(50%)
Clinico-pathological correlation	4(5%)
Required rotation	1(1%)
Elective rotation	7(9%)
Clinical resources	3(4%)
Gross/Micro examination	16(22%)
"Residents assigned to the department of pathology"	1(1%)
"Shared experiences with pathology residents"	1(1%)
Obtain copies of autopsy reports	11(15%)
Other	15(20%)

Teaching/conferences (didactic, morbidity/mortality, tumor board, grand rounds, and multidisciplinary) were the most common requirement. Sixteen programs must perform gross/microscopic examination; ophthalmology requires 36 hours. Medical genetics trainees have a required pathology rotation. Elective rotations should be available for neuromuscular disease, child neurology, general surgery, neurological surgery, otolaryngology, and radiation oncology. Others included: collaborations with pathologists(11;15%), "access to microbiology laboratory"(1; 1%), and structured experiences in blood banking and tissue banking"(1;1%).
Conclusions: Pathology departments at academic centers are faced with significant institution-wide pathology education requirements for clinical ACGME programs. Studies are ongoing to determine the hours required to fulfill these mandates (estimated at Duke as 4,500 + hours) and to develop innovative educational tools to satisfy the requirements and make efficient use of pathology teaching faculty.

502 Partners in Pathology: A Model for Department-Wide Educational Experience
W Foo, JW Carlson, E Lyon, D Walton, P Farmer, V Nose. Brigham and Women's Hospital, Boston, MA.
Background: Disease variety in large, tertiary care hospitals is often dictated by the demographics in which these hospitals operate. In order to broaden the overall educational experience in these settings, drawing upon clinicians in other settings must be pursued. Partners in Health is a comprehensive, community-based healthcare organization with clinics in seven countries. Although the disease burden in these settings is primarily infectious, the variety amongst benign and malignant neoplasms is diverse. The collaborative effort between our Department and Partners in Health serves an important role in alleviating health disparities for underserved patients and provides an overlooked opportunity to diversify and broaden educational experiences.
Design: To establish collaboration with clinicians working on-site, to demonstrate the ease of providing pathology services in resource poor settings, and to evaluate the exposure of our staff to different pathology.
Results: Sixty-four consecutive cases from Haiti, Rwanda, and Lesotho from patients with a median age of 27 (range 1-81) were examined. Diagnoses included twenty-five malignancies, eight infectious or inflammatory cases, and other rare entities. The malignancies included two uncommon cases of Kaposi sarcoma with lymphangiomatoid features, a case of malignant teratoid medulloepithelioma, and a case of extranodal sinusoidal histiocytosis. In addition, multiple EBV-associated neoplasms were demonstrated. Among the infectious cases were two cases of tuberculosis, a case of chromoblastomycosis, a case of actinomyces, and several cases with necrotizing granulomas where no organisms were identified. These cases were frequently presented at various department-wide conferences.
Conclusions: The diversity in non-infectious and infectious diseases represented an invaluable educational experience for our Department. In this cohort, many of the malignancies have been rarely reported in literature. These unusual cases served to educate both our trainees and our senior staff. The collaboration between an academic pathology department and clinicians operating in these resource poor settings was simple and brought with it a host of benefits to both parties.

503 High-Tech or High-Time to Re-Construct? What Type of First Impression Is Your Program Website Giving Prospective Applicants?
KA Hutchens, M Dahiya. Loyola University Medical Center, Maywood, IL.
Background: Previous studies have demonstrated that pathology residency applicants obtain much of their information, and thus the first impression of a program, from institutional websites. This study examined pathology program website accessibility and usefulness, in particular, features that may be alluring to perspective applicants.
Design: Current programs and web addresses were obtained from the Fellowship and Residency Electronic Database (FREIDA) list of graduate medical education programs under the pathology specialty section. The hyperlink from the database was used to access individual program websites. An average of fifteen minutes was spent per webpage, assessing fifteen individual content features, ranging from salary and curriculum, to interactive blogs and streaming video.
Results: 86.0% (129/150) of the programs had functioning web pages accessible via database hyperlink and 98.4% (127/129) had a detailed program description. The most common features were an outline of educational curriculum 89.9% (116/129), faculty biographies 68.2% (88/129), listing of current residents 64.3% (83/129), Electronic Residency Application Site (ERAS) link 63.5% (82/129), description of research opportunities 62.7% (81/129), and admissions requirements 62.7% (81/129). The least commonly seen features included resident evaluations 12.4% (16/129) and date/time stamps. 40.3% (52/129). 33.3% (43/129) included high-tech or interactive features such as blogs and streaming video.
Conclusions: Technology and the internet are prevalent in medical and resident education. Pathology programs need to demonstrate an interest and commitment to technology through high (100%) internet accessibility, as well as informative and stimulating site content designed to heighten applicant interest.

504 Digital Games Designed for Pathology Education
R Kanthan. University of Saskatchewan, Saskatoon, Saskatchewan, Canada.
Background: Computer-savvy 'net generation' students think and learn in different ways. Incorporation of such technologies within the confines of their education will enhance their educational experience. Digital gaming is an effective, enticing and encouraging way of learning. As pathology teaching hours compete for continued curricular representation, specially designed digital games for pathology education offers an alternative resource to complement the traditional teacher-led activities for the extended learning environment.
Design: Principles underlying game design construction included components of strategic thinking, interpretative analysis, and problem solving thereby contextually bridging the gap between the theory and application of pathology in a fun, entertaining game-like atmosphere. Use centered games were constructed with high time-on-task activities with motivation/goal orientation through rewards, clues, hints and partial solutions to keep progressing and self directing their own learning.
Results: Three educational games were designed with varying levels of complexity for the 'new' incoming first year medical, dental and physical therapy students and second year medical students. Game#1 – WORD SCRAMBLE AIM: To familiarize, improve vocabulary and gain expertise in the 'new' language of pathology. Game#2 – THE PATH IS RIGHT AIM: To provide a selected review sampling of midterm exam test materials in a fun game like atmosphere Game #3 – PATH TO SUCCESS Aim: To provide a comprehensive review sampling of final exam test materials in a fun game like atmosphere. 10 modified questions from this pool were evaluated in the written examination. Feedback was obtained via a semi-structured survey questionnaire. The notion of an electronic game format as an exam review was well received by students